

2010-01-01

Combustion Characteristics Of AlH₃ Flame

Sudipa Sarker

University of Texas at El Paso, ssarker@miners.utep.edu

Follow this and additional works at: https://digitalcommons.utep.edu/open_etd



Part of the [Mechanical Engineering Commons](#)

Recommended Citation

Sarker, Sudipa, "Combustion Characteristics Of AlH₃ Flame" (2010). *Open Access Theses & Dissertations*. 2779.
https://digitalcommons.utep.edu/open_etd/2779

This is brought to you for free and open access by DigitalCommons@UTEP. It has been accepted for inclusion in Open Access Theses & Dissertations by an authorized administrator of DigitalCommons@UTEP. For more information, please contact lweber@utep.edu.

COMBUSTION CHARACTERISTICS OF AlH_3 FLAME

SUDIPA SARKER

Department of Mechanical Engineering

APPROVED:

Ahsan R. Choudhuri, Ph.D., Chair

John F. Chessa, Ph.D.

Felicia S. Manciu, Ph.D.

Patricia D. Witherspoon, Ph.D.

Dean of the Graduate School

Copyright
by
Sudipa Sarker
2010

Dedication

This thesis is dedicated to my parents

COMBUSTION CHARACTERISTICS OF AlH_3 FLAME

by

Sudipa Sarker

THESIS

Presented to the Faculty of the Graduate School of

The University of Texas at El Paso

in Partial Fulfillment

of the Requirements

for the Degree of

MASTER OF SCIENCE

Department of Mechanical Engineering

THE UNIVERSITY OF TEXAS AT EL PASO

May 2010

Acknowledgement

I would like to acknowledge my advisor and mentor Dr. Ahsan Choudhuri for providing me with the opportunity and encouragement to follow my academic pursuits. I'd also like to recognize the Missile Defense Agency for providing the funding for this research. However, any opinions, findings, conclusions, or recommendations expressed herein are those of the author and do not necessarily reflect the view of the Missile Defense Agency.

Abstract

The combustion characteristics of Al hydride and Al were compared using a combustion chamber. Burning rate, ignition energy and temperature at atmospheric temperature and pressure in carbon dioxide and O₂ were tested with a volumetric flow rate that ranged from 10 to 50% in Ar. A spark ignition system was used to ignite the Alane and Aluminum. The combustion rate was measured using a high speed camera. Results showed the combustion rate of Alane and Aluminum decreases with increasing volumetric flow rate of oxidizer. And the combustion rate of Alane is higher than that of Aluminum. Alane needs more ignition energy than Aluminum to burn, which was measured using a high voltage probe and multimeter. A scanning electronic microscope (SEM) was used to obtain the morphology of the sample before the experiment to ensure the sample was pure enough to conduct the experiment. SEM was also used to obtain the morphology after burning to investigate the change in morphology. EDAX analysis was completed to obtain the quantitative analysis of the element and find the O₂ content before the experiment, which is the indication of purity in the sample. EDAX analysis was also completed after the experiment to obtain the percentage of O₂, which indicates the efficiency of the combustion reactions because O₂ is one of the main products after combustion. Flame evolution from high speed camera and thermal camera images suggest that flame quality Alane is better than that of Al in each condition. The flame temperature measured by K type thermocouple indicates flame temperature of Alane is higher than Aluminum for a given condition.

Table of Contents

1.0Introduction	1
1.1Physical Properties of Alane.....	1
1.2Research Objectives.....	3
1.3Determination of Combustion Properties	3
1.4Thesis Organization	3
1.5Center for Space Exploration Research Technology	4
2.0Background	6
2.2Methodology	8
3.0Experimental Facilities.....	9
3.1Combustion Chamber	9
3.2System Components	10
3.2.1Minimum Ignition Energy Circuit	10
3.2.2Weight measuring equipment	11
3.2.3Power Supply	12
3.2.4High Speed Camera	12
3.2.5Lab VIEW for Emission Spectra Analysis	12
3.3Flow Measurement Devices and Data Acquisition.....	13
3.3.1Flow Meter.....	13
3.3.2Metering and Shutoff Valves	15
3.4Scanning Electronic Microscope and EDAX	16

3.5Temperature Measurement	16
4.0Results and Discussion	18
4.1Physical Characterization of Sample before Experiment	18
4.2Determination of Burning Time	22
4.3 Physical Characterization of Burned AlH ₃ and Al.....	26
4.4Determination of Minimum Ignition Energy	36
4.5Flame Evolution.....	39
4.67.Determination of Burning Time Using Emission Spectra of AlO.....	41
5.0Conclusions	45
6.0References	50
Curriculum Vita.....	52

List of Figures

Fig 3.1 Experimental Setup.....	10
Fig 3.2 Experimental Setup for Minimum Ignition Energy.....	11
Fig 3.3 OHAUS AV53 Adventurer Pro Precision Balance	11
Fig 3.4 LOKO-Power Supply DPS-3050	12
Fig 3.5 PHOTRON FASTCAM-Super 10K High Speed Camera.....	12
Fig 3.6 Lab VIEW VI File with Front Panel and Block Diagram	13
Fig 3.7 Digital Mass Flow Meter	14
Fig 3.8 Dry Cal Calibrator	14
Fig 3.9 Swagelok SS-SS4VH Metering Valve 1	15
Fig 3.10 Swagelok SS-4P4T4 Shutoff Valve 1	15
Fig 3.11 Scanning Electronic Microscope	16
Fig 3.12 Set up for Thermocouple Measurement	17
Fig 4.1 Percentage of O ₂ in AlH ₃ sample	18
Fig 4.2 Percentage of O ₂ in Al	19
Fig 4.3 Percentage of O ₂ in Al	20
Fig4.4 SEM image of the AlH ₃ sample at different magnifications	21
Fig4.5 SEM image of the Al sample.....	21
Fig 4.6 Burning Time of AlH ₃ with CO ₂ in Ar	22
Fig 4.7 Burning Time of AlH ₃ with CO ₂ in Ar	22
Fig 4.8 Burning Time of Al with CO ₂ in Ar	23
Fig4.9 Burning Time of Al with CO ₂ in Ar	23

Fig 4.10 Comparison of Burning Time of Al H ₃ using Different Oxidizers (O ₂ ,CO ₂)...	24
Fig 4.11 Comparison of Burning Time of Al H ₃ and Al using CO ₂	24
Fig 4.12 Comparison of Burning Time of AlH ₃ and Al using O ₂	25
Fig 4.14 Percentage of O ₂ Conversion for AlH ₃ with 10% of CO ₂ in Ar.....	26
Fig 4.15 Percentage of O ₂ Conversion for Al with 10% of CO ₂ in Ar.....	27
Fig 4.16 Percentage of O ₂ Conversion for AlH ₃ with 20% of CO ₂ in Ar.....	28
Fig 4.17 Percentage of O ₂ Conversion for Al with 20% of CO ₂ in Ar.....	29
Fig 4.18 Percentage of O ₂ Conversion for AlH ₃ with 30% of CO ₂ in Ar.....	30
Fig 4.19 Percentage of O ₂ Conversion for Al with 30% of CO ₂ in Ar.....	31
Fig 4.20 Percentage of O ₂ Conversion for Al H ₃ with 40% of CO ₂ in Ar.....	32
Fig 4.21 Percentage of O ₂ Conversion for Al with 40% of CO ₂ in Ar.....	33
Fig4.22 Percentage of O ₂ Conversion for AlH ₃ and Al with CO ₂ in Ar.....	34
Fig 4.23 SEM images of burned AlH ₃ and Al.....	35
Fig 4.24 Comparison of Minimum Ignition Energy to Burn AlH ₃ using (O ₂ and CO ₂)	36
Fig 4.25 Comparison of Minimum Ignition Energy of Al H ₃ and Al Using CO ₂	37
Fig 4.26 Comparison of Minimum Ignition Energy to Burn AlH ₃ and Al Using O ₂	37
Fig 4.27 Comparison of Minimum Ignition Energy of AlH ₃ and Al using (O ₂ and CO ₂).....	38
Fig 4.28 Flame Evolution using High Speed Camera.....	39
Fig 4.29 (c) AlH ₃ Flame with 10% O ₂ in Ar	40
Fig 4.29 (d) Al Flame with 10% O ₂ in Ar.....	40
Fig 4.30 Emission Spectra of AlH ₃ Flame using 10% CO ₂ in Ar	41

Fig 4.31 Emission spectra of Al flame using 10% CO ₂ in Ar.....	42
Fig 4.32 Emission spectra of AlH ₃ and Al flame using 20% CO ₂ in Ar	43
Fig 4.33 (a) Temperature of AlH ₃ flame using 50% CO ₂ in Ar	44
Fig 4.33 (b) Temperature of Al Flame using 50% CO ₂ in Ar.....	44

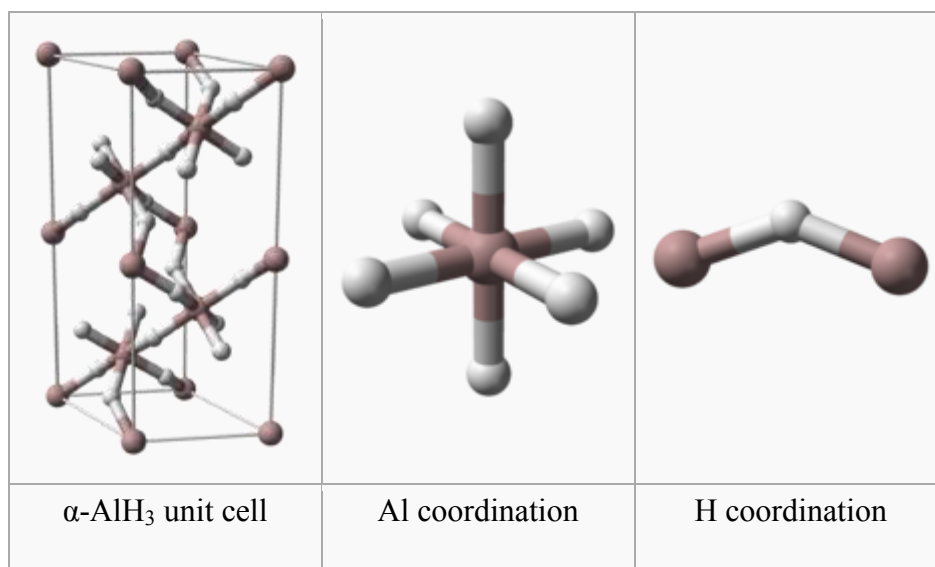
1.0 Introduction

1.1 Physical Properties of Alane

The key requirements for any candidate hydrogen storage material in automotive applications are high gravimetric and volumetric hydrogen densities, a release of hydrogen at moderate temperatures and pressures, and a low-cost method to recharge the material back to its original state. Aluminum hydride or Alane (AlH_3) has been investigated as a possible substitute for Aluminum (Al) in solid rocket motor (SRM) propellants. AlH_3 is a covalent binary hydride that has been known for more than 60 years as an attractive medium for on-board automotive hydrogen storage [1]. AlH_3 is a fuel of relatively low density (1.477 g/cm^3) and large molecular mass (30.01 g/mole). Density of AlH_3 is significantly less than that of Al (2.70 g/cm^3). AlH_3 consists of about 10% hydrogen by mass, thereby providing a higher density of hydrogen ($0.148 \text{ gH}_2/\text{cm}^3 \text{ AlH}_3$) than liquid hydrogen. The low density makes AlH_3 more convenient for applications in upper-stage and space motors [2].

AlH_3 is stable at room temperature despite having an equilibrium hydrogen pressure of between 1 and 10 kbar at 298K. The stability is generally attributed to a surface oxide layer, which acts as a kinetic barrier to decomposition and protects the AlH_3 from the environment. [3, 4]

There are at least 7 non-solvated AlH_3 phases Al hydride is formed as numerous polymorphs: α -alane, α' -alane, β -alane, δ -alane, ϵ -alane, θ -alane, and γ -alane. α -alane has a cubic or rhombohedral morphology [5]. The structure of α -alane has been determined and contains Al atoms surrounded by 6 hydrogen atoms that bridge to 6 other Al atoms. The Al-H distances are all equivalent (172 pm) and the Al-H-Al angle is 141° . [6]



α -Alane is the most thermally stable polymorph. β -alane and γ -alane are produced together, and will turn into α -alane upon heating [6].

High degree of energy release from the combustion of both Al and hydrogen along with the above properties make alane an ideal additive for solid propellants. Replacing Al with alane will result in at least a 10% gain in specific impulse over currently used SRM propellants. The greater temperature stability and longer shelf life of α -AlH₃ will likely make it the preferred polymorph for automotive fuel cell applications. [2]

Experiments were conducted to establish that the burning characteristics of AlH₃ are similar to Al or better than Al. If the burning characteristics of the two materials are similar or if the burning characteristics of AlH₃ are better than Al, then the replacement of Al with AlH₃ in energetic materials applications would be warranted.

1.2 Research Objectives

Physical characterization

Morphology

SEM (Scanning Electronic Microscope) Analysis was done to get the morphology of sample (AlH₃ and Al) and burned samples (AlH₃ and Al)

Elemental Composition

EDAX analysis was done to get quantitative measurements (elemental analysis) of the sample(measurement of purity) and burned samples to get percentage conversion of O₂ which is the indication of the efficiency of the combustion reaction

1.3 Determination of Combustion Properties

- Flame evolution is observed by high speed camera and thermal camera using the following oxidizers.
$$\text{AlH}_3 + (\text{CO}_2 + \text{Ar}) [\text{Ar: 10\%-50\% by volume}]$$
$$\text{AlH}_3 + (\text{O}_2 + \text{Ar}) [\text{Ar: 10\%-50\% by volume}]$$
- Determination of Burning time of AlH₃ and Al using high speed camera (stability period of the flame).
- Determination of burning time using the emission spectra of AlO (monochromator).
- Determination of minimum Ignition energy using high voltage probe and multimeter.

1.4 Thesis Organization

Chapter 1 provides an outline provides regarding the chemical structure and physical properties of AlH₃ which properties make AlH₃ an ideal additive to solid rocket propellant and the objective of the research.

Chapter 2 provides a summary of the technical background on hypothetical basis by which conclusions of the experimental data will be drawn.

Chapter 3 provides an outline of the detailed experimental setup in determining the burning time, ignition energy, physical characteristics (scanning electronic microscopic image to get the morphology and EDAX analysis to get the quantitative analysis of the sample)

Chapter 4 presents the data regarding the burning time, ignition energy, morphology and quantitative analysis of the sample and burned sample

Chapter 5 concludes the combined results.

1.5 Center for Space Exploration Research Technology

The Center for the Space Exploration Technology Research (cSETR) (formerly the Combustion and Propulsion Research Lab) is located in Mechanical Engineering Department at The University of Texas at El Paso. The Center provides computational and experimental research related to the field of combustion, fluid mechanics and propulsion with a wide range of software and equipment. The primary focus of the research is in the development of micro-propulsion and micro-combustion technologies. The Center also provides a collection of optical instrumentation; high speed cameras; an intensified charge-coupled device (CCD) camera; laser based measurement techniques, such as particle image velocimetry (PIV); and a vacuum chamber to replicate the space atmosphere, which completes the necessary equipment for propulsion systems development. Current fluid dynamics instrumentation includes a laser doppler velocimeter (LDV), a PIV, a stereo particle image velocimetry, a high speed particle image velocimeter (HPIV), a multi-channel hotwire (thermal) anemometry system, a spectroscopy system (imaging spectrograph; detectors; control and gating electronics), thermal

imaging systems, intensified high speed camera, various flow controllers, flow meters, and high speed data acquisition systems.

2.0 Background

2.1 Literature Review

AlH₃ is a well-known reducing agent which is very much useful for wide range of applications (in solid or hybrid rocket propulsion, hydrogen storage material, hydrogen source for fuel cells, polymerization catalysis, etc). In space applications, AlH₃ gives high energy from the oxidation of metal and low molecular weight due to the hydrogen which results in optimum performance [7]. There are some techniques that can produce phase-pure α -AlH₃ in Russia and USA. [8]

Compatibility of materials is also an important factor. Many testing is going on to make sure whether AlH₃ can be stable after it's mixing with fuel and other additives [9]. Pure Al has a γ oxide coating that gives low temperature inertness in bulk Al, but in case of AlH₃ particles, the activity of the oxide is dependant on the specific stabilization process stabilization [8,10].

A very few experiments were conducted for Combustion data on Al hydride. Selezenev et al. [11] compared various effects of Al and Al hydride on the detonation and composite explosives' performance using some models and experimental results.

Il'in et al. [12] some research on the combustion of Al hydride in air at 1 atm. Al hydride was burned in a same method which is similar to elemental Al except for an hydrogen combustion which occurs low temperatures.

The most stable form is α -alane which has been used in the current investigation. Brower et al. [13] reported that Al hydride synthesis, the β -alane and γ -alane forms were formed firstly in the final steps; they were converted to α -alane after heating. Polarizing-light microscopy showed the crystals of the α -alane phase were mostly hexagonal and cubical.

In respect to combustion time and temperature at elevated pressures in different oxidizers (carbon dioxide and O₂ has been), a comparison of combustion characteristics between Al hydride and Al has been done using a shock tube. The combustion time of 5-10 micron Al hydride is very similar to that of Al for a specific volumetric flow rate of oxidizer. [2]

The ignition process caused by electric spark has two theories: electrical model and thermal model. Sparks: The electrical model says that the transport of chemical energy is occurred by the internal diffusion of reactants and reaction products, and thermal model considers the transport of the thermal energy i.e. heat. [14]

Since there are few studies regarding the combustion of Al hydride, there exists the need to establish the burning characteristics of alane in order to consider it for applications where it would replace Al. If the burning characteristics of the two materials are similar or burning characteristics of ALH₃ are better than Al. Here the experiments were conducted to establish that the burning characteristics of AlH₃ are similar to Al or better than Al. If the burning characteristics of the two materials are similar or if the burning characteristics of alane are better than Al, then the replacement of Al with AlH₃ in energetic materials applications would be warranted.

2.2 Methodology

A design of experiments has been generated to determine the burning rate, ignition, morphology and quantitative elemental analysis of sample and to get the morphology and quantitative elemental analysis after the sample is burned. K type thermocouple used to get the flame temperature. High speed camera used to get the burning time. Thermal camera and high speed camera used to get the evolution of the flame. Multimeter and high voltage probe used to get the minimum ignition energy. Scanning electronic microscope and EDAX used to get the morphology and elemental quantities. 1 mg of sample used for each experiment and to burn the sample, the following oxidizers were used.

$\text{AlH}_3 + (\text{CO}_2 + \text{Ar})$ [Ar: 10%-50% by volume]

$\text{AlH}_3 + (\text{O}_2 + \text{Ar})$ [Ar: 10%-50% by volume]

3.0 Experimental Facilities

3.1 Combustion Chamber

Combustion chamber was made out of solid stainless steel rod. A hole of 4 mm dia and 4 mm height was made for the purpose of Combustion inside the combustion chamber. Two holes were made in the opposite direction on the face of the chamber to connect the igniter. Another hole is made to insert the thermocouple. The igniter made of platinum wire was placed in such a way so that the spark generate at the base of the hole to make sure the contact of fuel with spark. Ceramic tubes were used for housing platinum wire to prevent arcing outside and inside the chamber walls. DC Power Supply, DPS-3050 was used to obtain a variable AC power across the igniter gap and in between a transformer was used to increase the AC output. Two more holes were also made on the faces of the chamber to deliver the oxidizer. All the gases (O_2 , CO_2 , and Ar) are stored separately in gas cylinders under 1600 psi pressure. The Purity of these gases is 99%. Different Flow meters are used in this experiment maintaining volumetric flow rate. Manual precision metering valves in conjunction with low-torque-quarter-turn plug valves are used to control O_2 , CO_2 , and Ar flow rate to the combustion chamber.

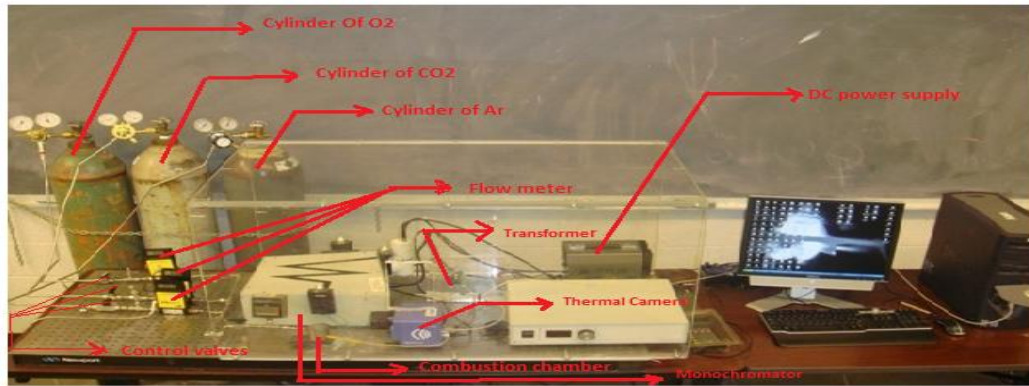


Fig 3.1 Experimental Setup

3.2 System Components

3.2.1 Minimum Ignition Energy Circuit

Voltage measurements were performed using a Fluke 80K-40 High Voltage Probe which was connected to a Fluke 187 True RMS Multimeter. Measurements were performed by connecting the transformer directly to the Fluke High Voltage Probe in parallel. The current measurements were performed using another separate Fluke 187 True RMS Multimeter.

The equation $P=I*V$ was used to calculate the power and then power converted to minimum ignition energy. The measurement had an equipment error of 0.4% of the measured value.

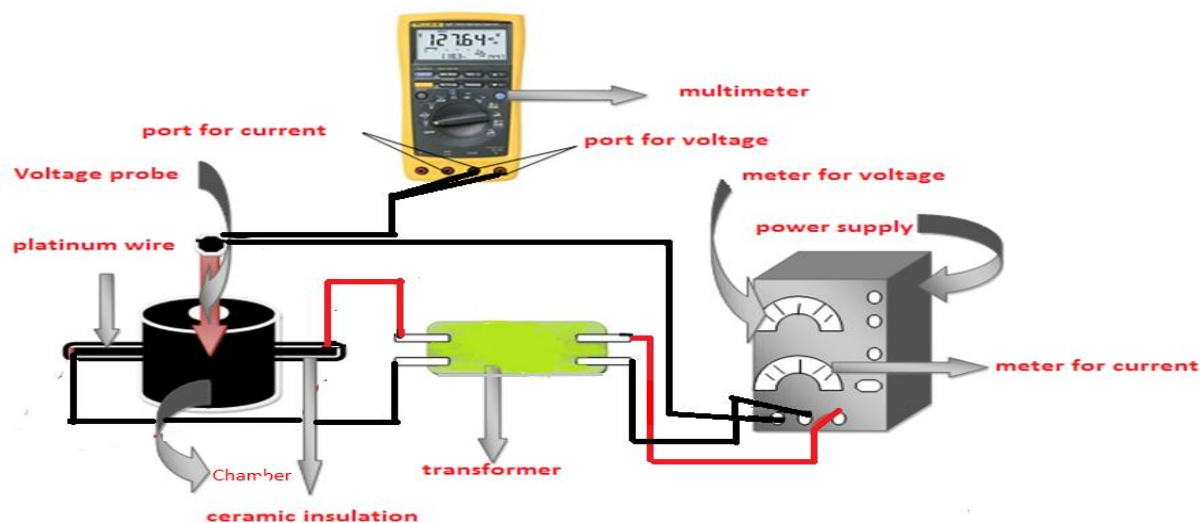


Fig 3.2 Experimental Setup for Minimum Ignition Energy

3.2.2 Weight measuring equipment

Since 1 mg of sample used in each experiment, the weight had to be measured with a precision balance (Fig 3.3) prior the execution of the experiment.



Fig 3.3 OHAUS AV53 Adventurer Pro Precision Balance

3.2.3 Power Supply

The system was powered by a DC power supply to ignite the sample.



Fig 3.4 LOKO-Power Supply DPS-3050

3.2.4 High Speed Camera

High speed camera was used to get the burning time and evolution of the flame. After recording the burning, the recording clip was used to get the burning time.



Fig 3.5 PHOTRON FASTCAM-Super 10K High Speed Camera

3.2.5 Lab VIEW for Emission Spectra Analysis

Lab VIEW version 8.2 is the computer software used to display and store the output signals from the AIO emission to get the burning time using the wavelength 486 nm.

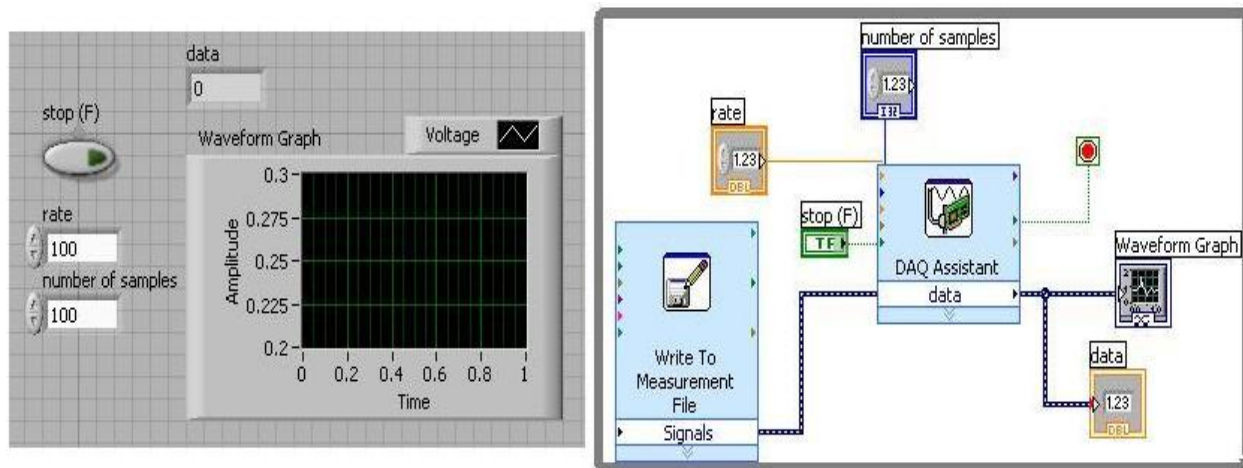


Fig 3.6 Lab VIEW VI File with Front Panel and Block Diagram

3.3 Flow Measurement Devices and Data Acquisition

3.3.1 Flow Meter

Digital flow meters (Omega FMA 1700/1800 series in Figure 3.7) were used to measure the volumetric flow rate of oxidizers. The specifications of the mass flow meters are: temperatures ranging from 0°C to 50°C, pressures up to 500 psig, relative humidity of 70%, and accuracy $\pm 1.5\%$ of full scale. Prior to each experiment, flow meters are calibrated by using Dry Cal Meter Calibrates as shown in Figure 3.8.



Fig 3.7 Digital Mass Flow Meter



Fig 3.8 Dry Cal Calibrator

3.3.2 Metering and Shutoff Valves

Manual precision metering valves (SS-SS4VH in Fig 3.9) in conjunction with low-torque-quarter-turn plug valves were used to control the volumetric flow rate of oxidizers. The Shutoff valves (SS-4P4T4 in Fig 3.10) were used to shut off the fuel flow from the pressurized gas cylinders.



Fig 3.9 Swagelok SS-SS4VH Metering Valve 1



Fig 3.10 Swagelok SS-4P4T4 Shutoff Valve 1

3.4 Scanning Electronic Microscope and EDAX

Characteristics information of SEM is

- Topography:** The Surface feature of an object that is object's texture.
- Morphology:** Shape and size of the particles
- Composition:** The elements of the object and their quantitative measurement
- Crystallographic Information:** How the atoms are arranged in an object



Fig 3.11 Scanning Electronic Microscope

3.5 Temperature Measurement

K type thermocouple used to get the temperature.

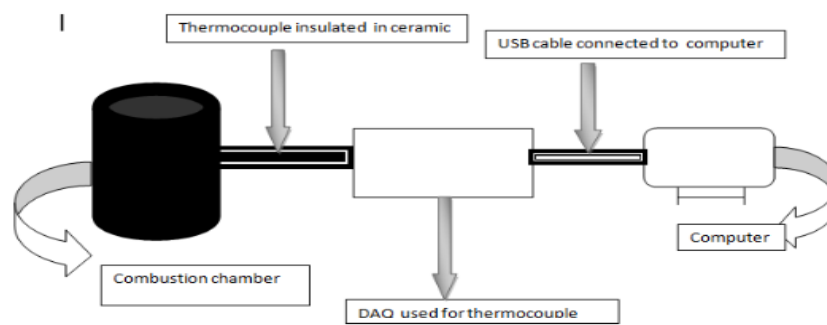


Fig 3.12 Set up for Thermocouple Measurement

4.0 Results and Discussion

4.1 Physical Characterization of Sample before Experiment

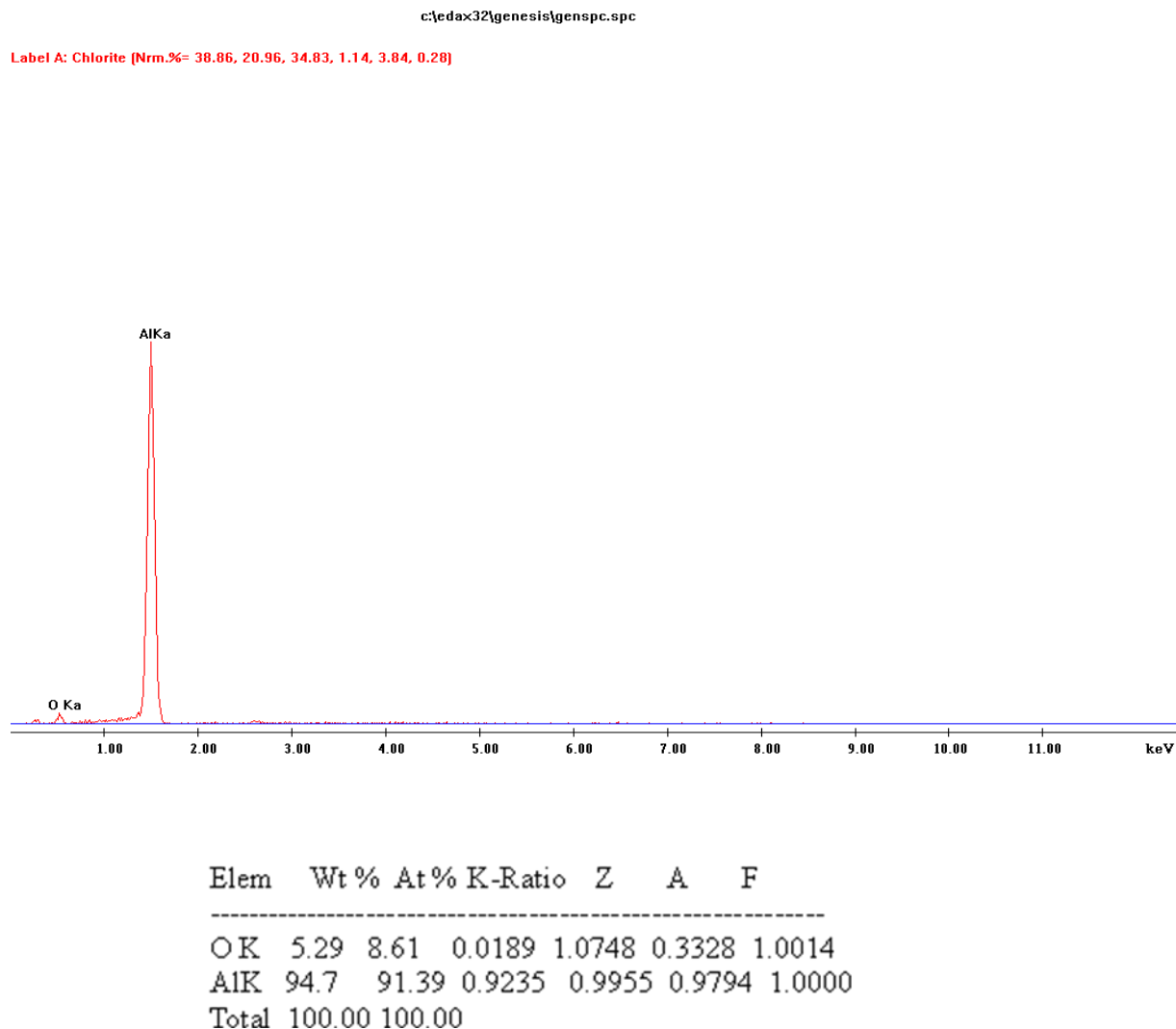
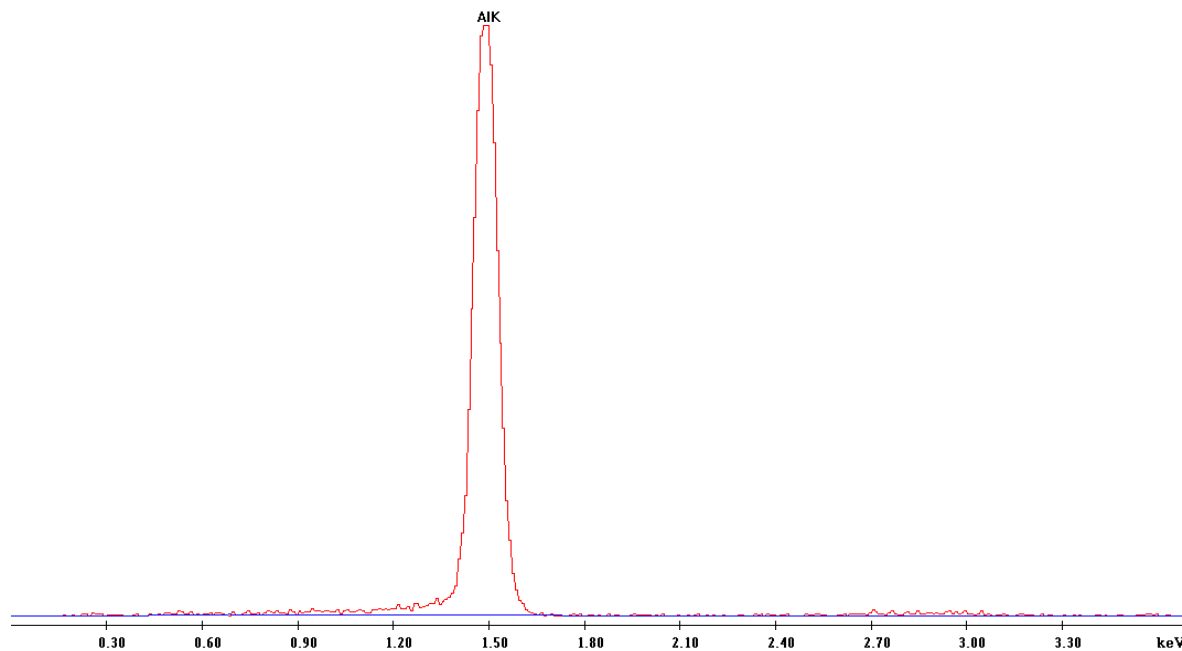


Fig 4.1 Percentage of O2 in AlH3 sample

EDAX analysis of the sample indicates that the sample, AlH3 contains only 5 percent of O2. Since the amount of O2 is negligible, the sample is pure enough to conduct the experiment

Label A: Chlorite [Nrm.%= 38.86, 20.96, 34.83, 1.14, 3.84, 0.28]

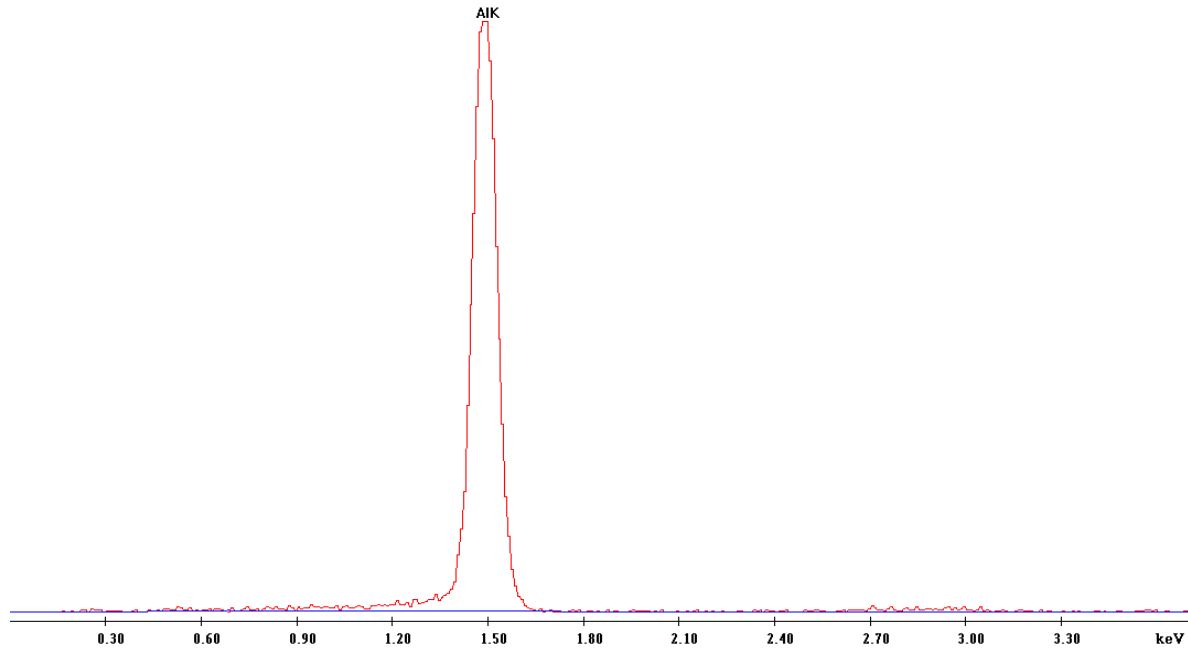


Elem	Wt %	At%	K-Ratio	Z	A	F
AlK	100.00	100.00	1.0000	1.0000	1.0000	1.0000
Total	100.00	100.00				

Fig 4.2 Percentage of O2 in Al

EDAX analysis of the sample indicates that the sample, Al contains no O2. Since there is no O2 in sample, the sample is pure enough to conduct the experiment

Label A: Chlorite [Nrm.%= 38.86, 20.96, 34.83, 1.14, 3.84, 0.28]



Elem	Wt %	At %	K-Ratio	Z	A	F
AlK	100.00	100.00	1.0000	1.0000	1.0000	1.0000
Total	100.00	100.00				

Fig 4.3 Percentage of O2 in Al

EDAX analysis of the sample indicates that the sample, Al contains no O₂. Since there is no O₂ in the sample, the sample is pure enough to conduct the experiment.

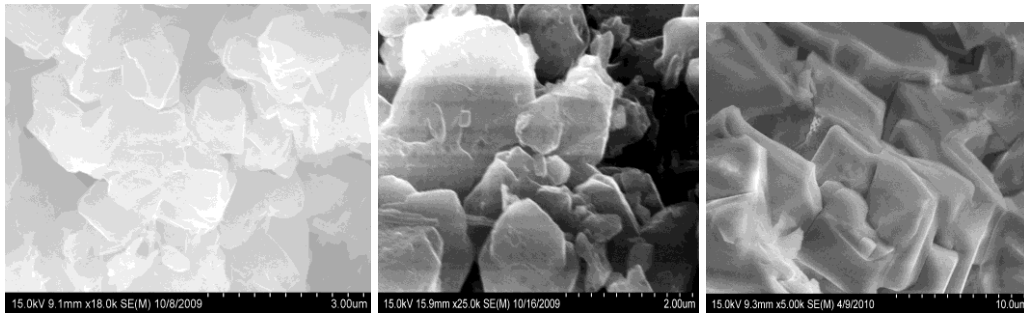


Fig4.4 SEM image of the AlH₃ sample at different magnifications

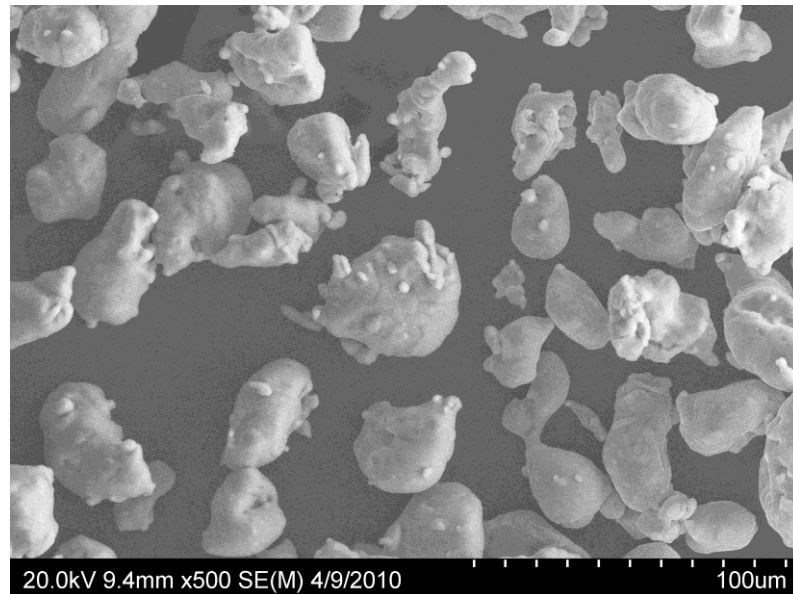


Fig4.5 SEM image of the Al sample

Figure 4.4 shows that the particles are mostly cubic crystal shapes. Cracks and pits are noted occasionally on the surface but these are not deep. The SEM size of the particles ranges between 1 and 15 μ m. It is also noted in the SEM images that most of the particles have smooth surfaces, which shows that AlH₃ particles are non-porous and have an insignificant level of porosity. Fig4.5 shows that the particles are not aggregated and spherical in shape.

4.2 Determination of Burning Time

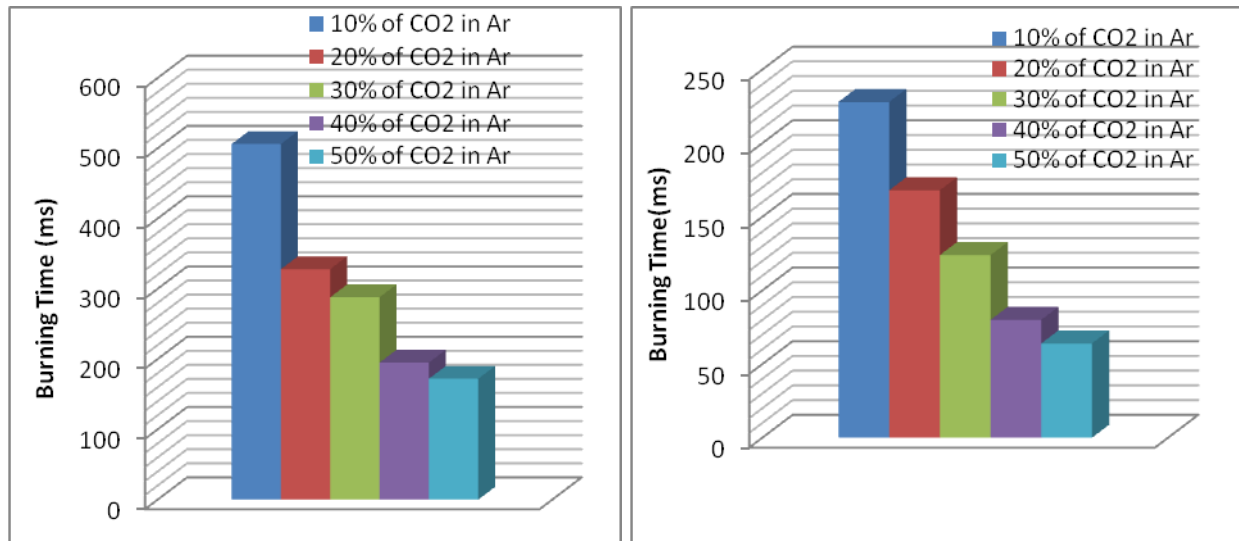


Fig 4.6 Burning Time of AlH3 with CO2 in Ar Fig 4.7 Burning Time of AlH3 with CO2 in Ar

Figures 4.6 and 4.7 show that the burning time (using high speed camera) of AlH3 decreases with increasing the volumetric flow rate of CO2 in Ar. Burning time of AlH3 is higher in CO2 than O2.

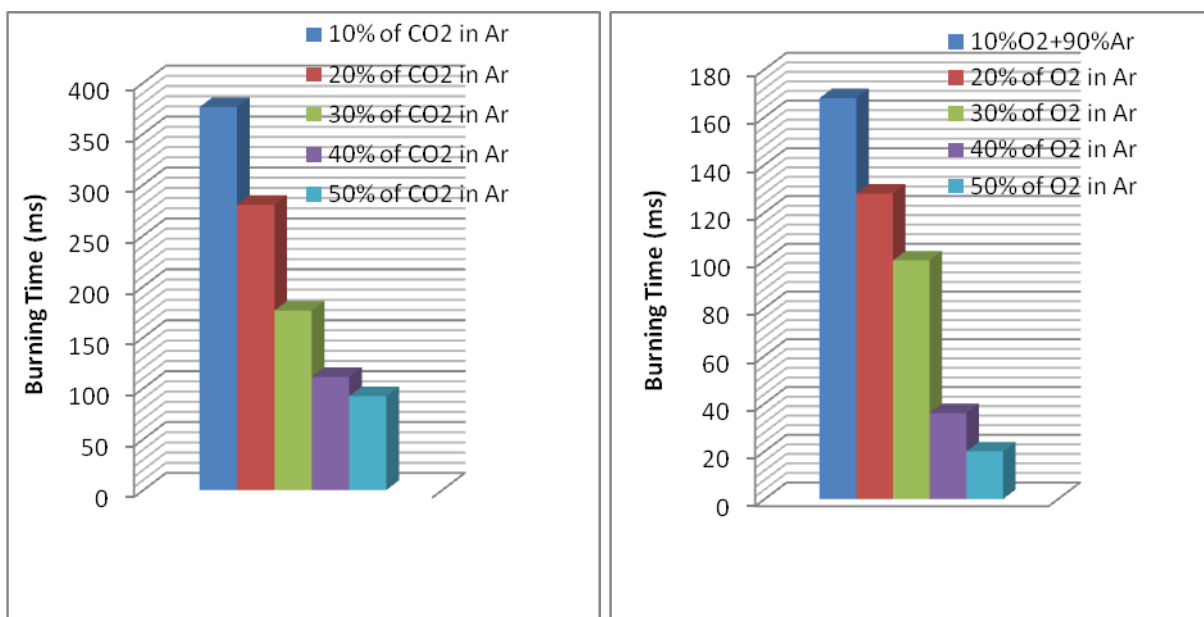


Fig 4.8 Burning Time of Al with CO2 in Ar Fig4.9 Burning Time of Al with CO2 in Ar

Figures 4.8 and 4.9 show that burning time (using high speed camera) of Al decreases with the increasing the volumetric flow rate of CO2 and O2 in Ar. Burning time of Al is higher in CO2 rather than O2.

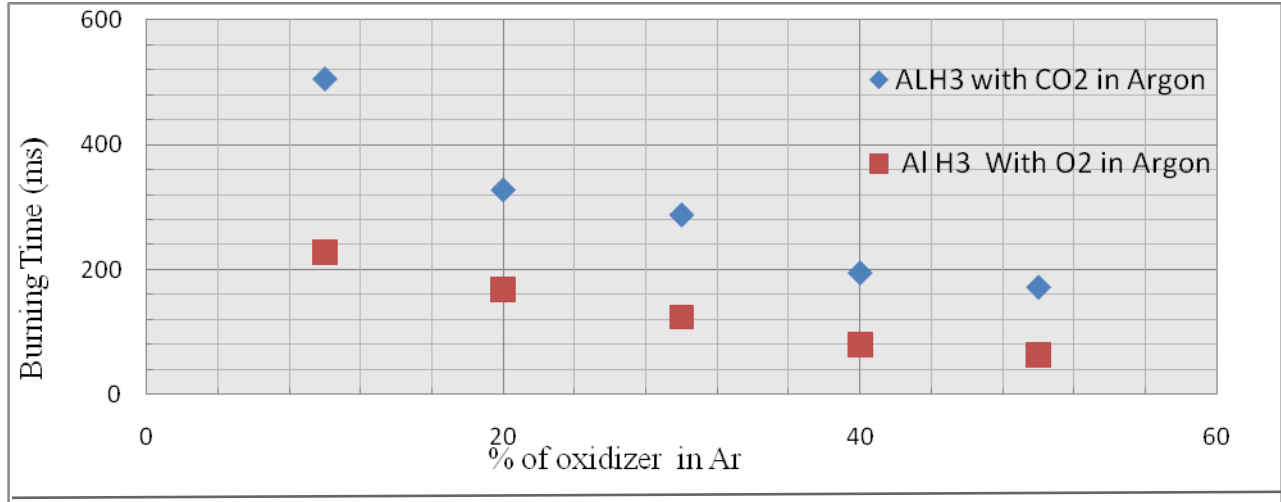


Fig 4.10 Comparison of Burning Time of Al H3 using Different Oxidizers (O2 and CO2)

Figure 4.10 shows that the burning time (using high speed camera) decreases almost linearly with increasing the volumetric flow rate of oxidizers in Ar for ALH3. Burning time of ALH3 is in CO2 rather than O2.

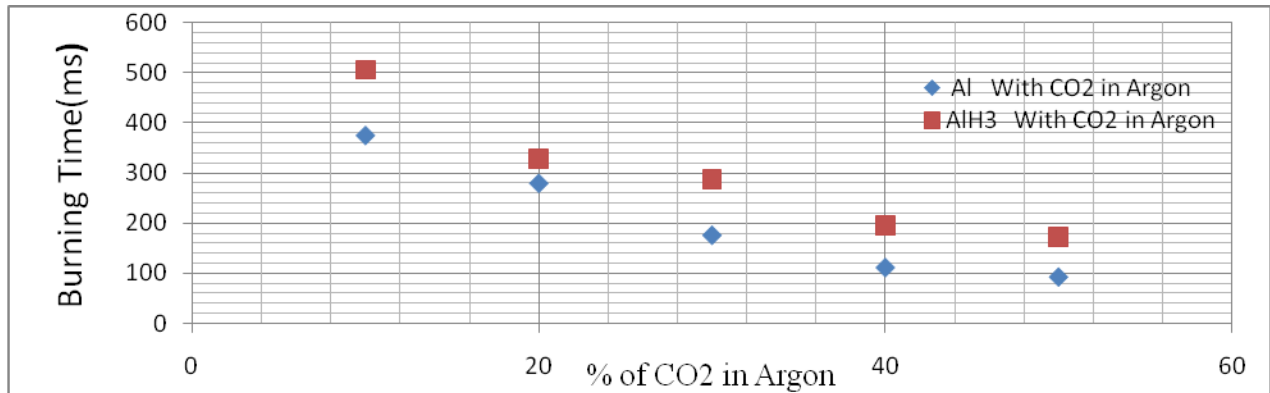


Fig 4.11 Comparison of Burning Time of Al H3 and Al using CO2

Figure 4.11 shows that burning time (using high speed camera) decreases almost linearly with increasing the volumetric flow rate of oxidizers in Ar for AlH₃ and Al. Burning time of AlH₃ is higher in CO₂ rather than Al in CO₂.

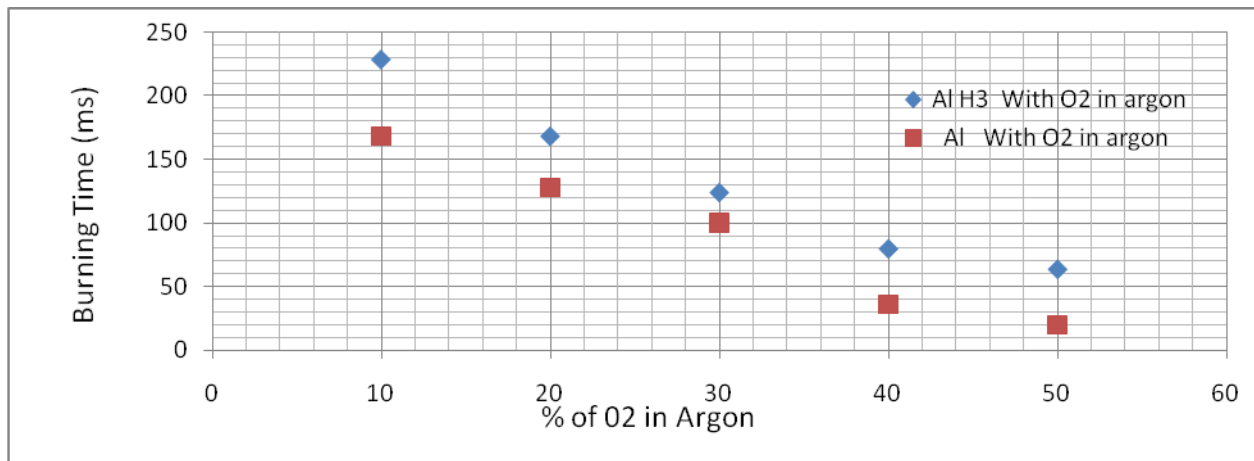


Fig 4.12 Comparison of Burning Time of AlH₃ and Al using O₂

Figure 4.12 shows that burning time (using high speed camera) decreases almost linearly with increasing the volumetric flow rate of oxidizers in Ar for AlH₃ and Al. Burning time of AlH₃ is higher in O₂ rather than Al in O₂.

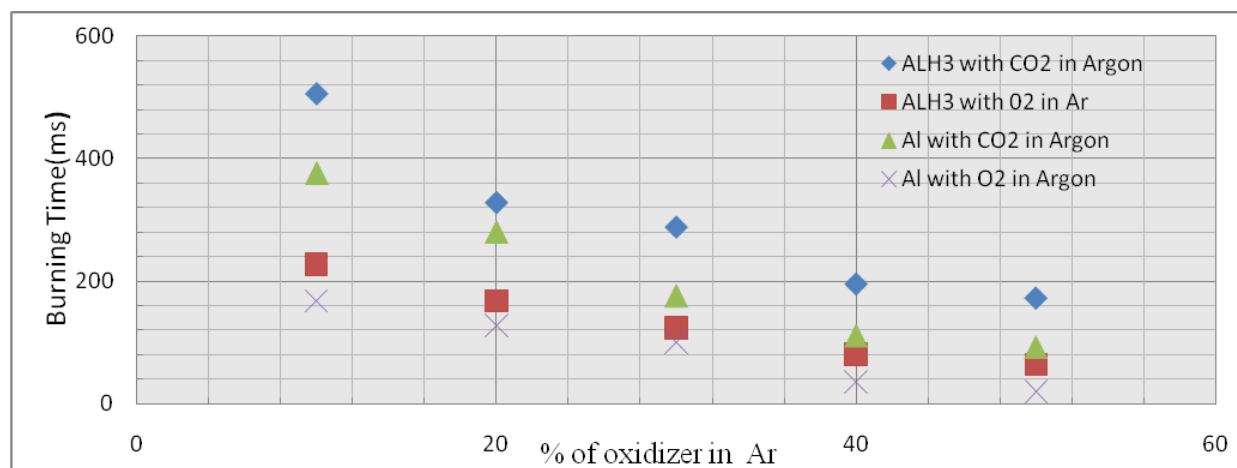
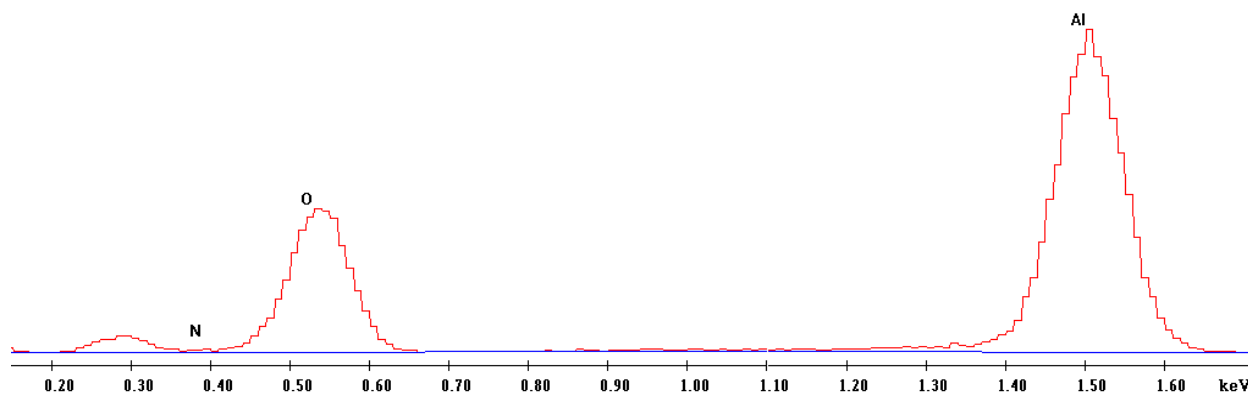


Fig 4.13 Comparison of Burning Time of AlH₃ and Al Using Different Oxidizers

Burning time (using high speed camera) decreases almost linearly with increasing the volumetric flow rate of oxidizers in Ar for AlH₃ and Al. Burning time of AlH₃ is higher than Al for all conditions.

4.3 Physical Characterization of Burned AlH₃ and Al

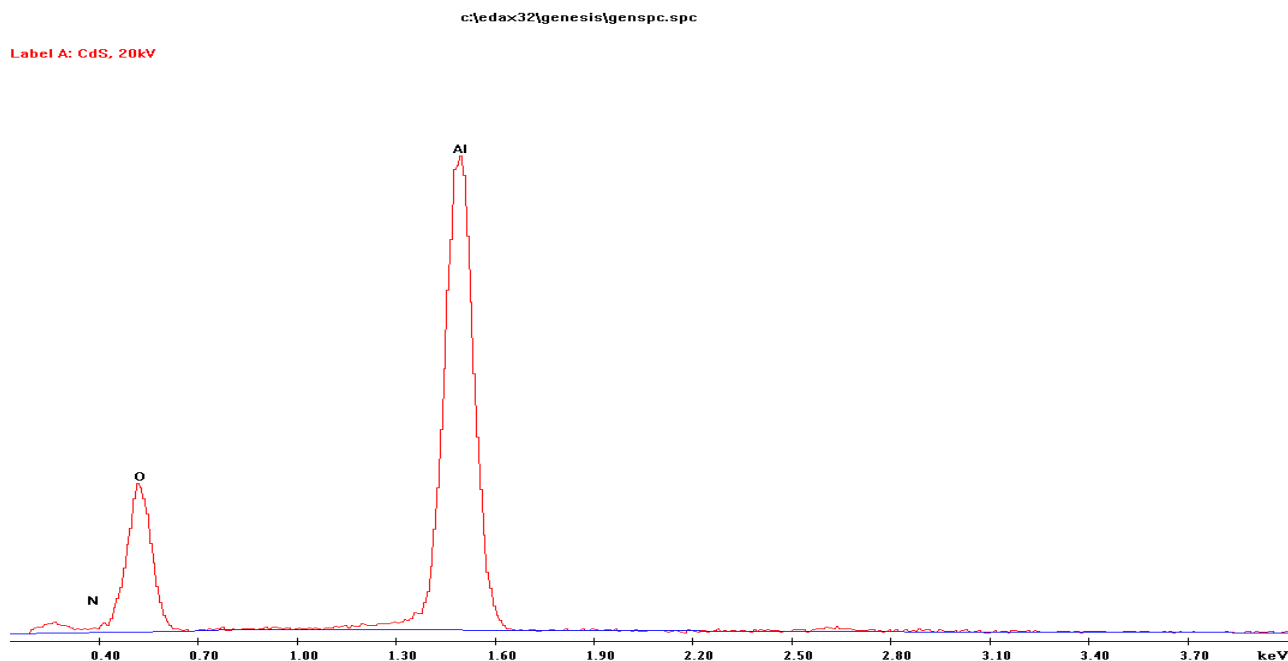


Elem Wt % at % K-Ratio Z A F

N	K	1.85	2.59	0.0049	1.04	O2 0.2545 1.00
O	K	52.27	64.07	0.2158	1.03	18 0.3998 1.00
Al	K	45.88	33.34	0.3182	0.96	10 0.7218 1.00
Total		100.00	100.00			

Fig 4.14 Percentage of O₂ Conversion for AlH₃ with 10% of CO₂ in Ar

Figure 4.14 shows that when AlH₃ is Burned with 10% of CO₂ in Ar, O₂ Conversion is 52.27%.



Elem Wt % at % K-Ratio Z A F

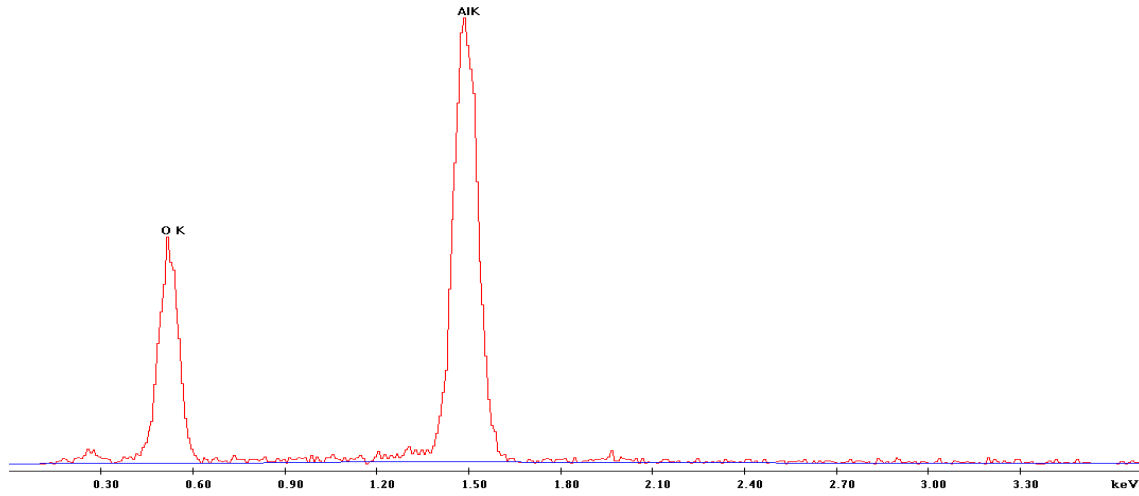
```
-----
N K 5.21 7.53 0.0126 1.0454 0.2303 1.0016
O K 41.55 52.55 0.1394 1.0370 0.3232 1.0008
AlK 53.23 39.92 0.3887 0.9657 0.7560 1.0000
Total 100.00 100.00
```

Fig 4.15 Percentage of O₂ Conversion for Al with 10% of CO₂ in Ar

Figure 4.15 shows that when AlH₃ is burned with 10% of CO₂ in Ar, O₂ conversion is 41.55%. So the O₂ conversion is higher for AlH₃ than Al with the same volumetric flow rate of oxidizer.

C:\Documents and Settings\skgullapalli\Desktop\April 9th\sample 10\sample 10.spc

Label A: Chlorite [Norm. %= 38.86, 20.96, 34.83, 1.14, 3.84, 0.28]



Elem Wt % at % K-Ratio Z A F

O K 45.03 58.01 0.2281 1.0414 0.4862 1.0007

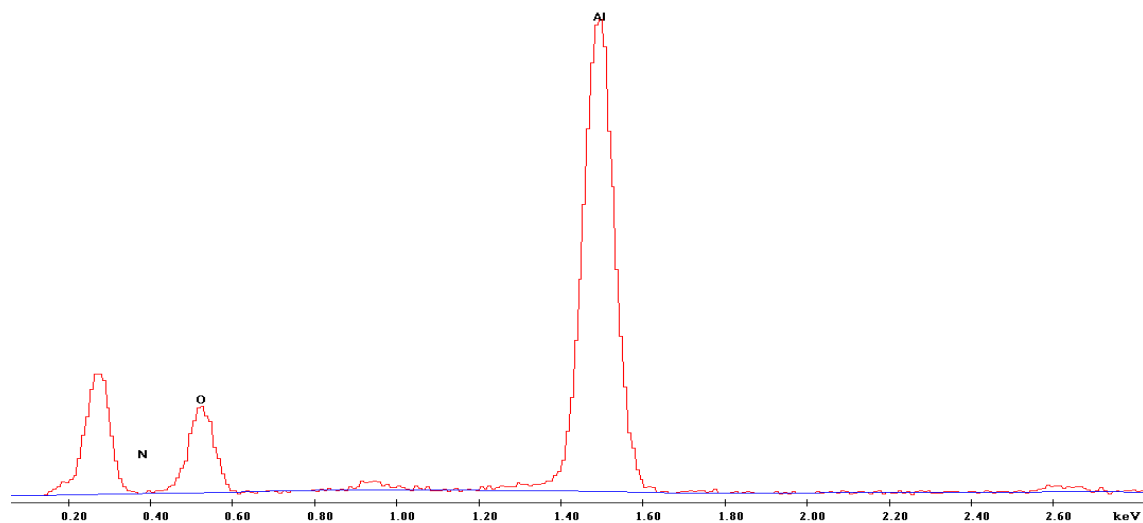
AlK 54.97 41.99 0.4472 0.9638 0.8442 1.0000

Total 100.00 100.00

Fig 4.16 Percentage of O₂ Conversion for AlH₃ with 20% of CO₂ in Ar

Figure 4.16 shows that when AlH₃ is burned with 210% of CO₂ in Ar, O₂ conversion is 45.03%.

Label A: Chlorite [Nrm.%= 38.86, 20.96, 34.83, 1.14, 3.84, 0.28]



Elem Wt % at % K-Ratio Z A F

N K 1.68 2.57 0.0036 1.0532 0.2041 1.0015

O K 35.26 47.28 0.1207 1.0447 0.3275 1.0009

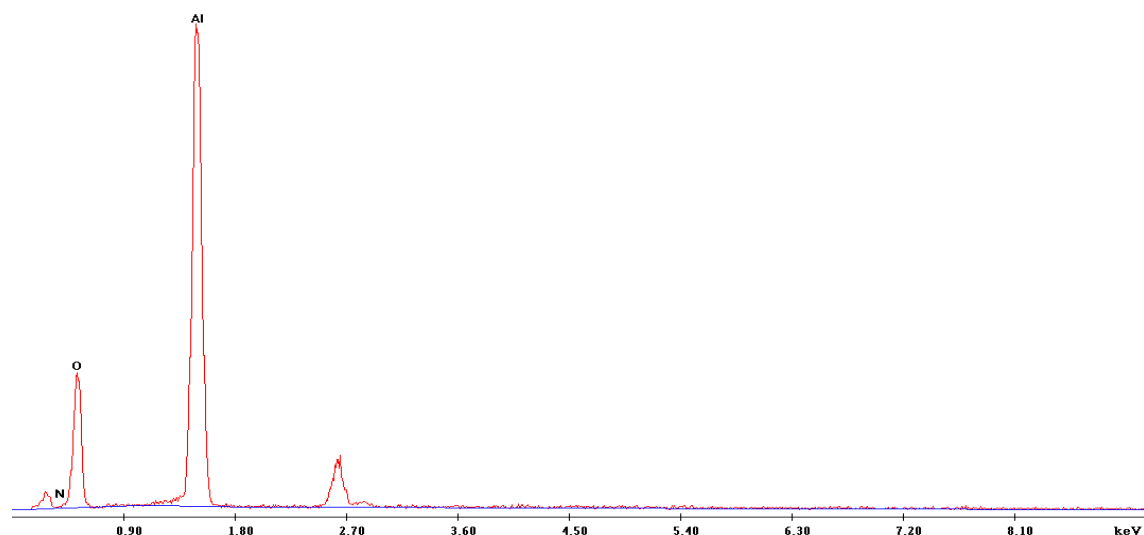
AlK 63.07 50.15 0.4884 0.9729 0.7960 1.0000

Total 100.00 100.00

Fig 4.17 Percentage of O₂ Conversion for Al with 20% of CO₂ in Ar

Fig4.17 shows that when AlH₃ is burned with 10% of CO₂ in Ar, O₂ conversion is 35.26%. So the O₂ conversion is higher for AlH₃ than Al with the same volumetric flow rate of oxidizer.

Label A: Chlorite (Nrm.%= 38.86, 20.96, 34.83, 1.14, 3.84, 0.20)



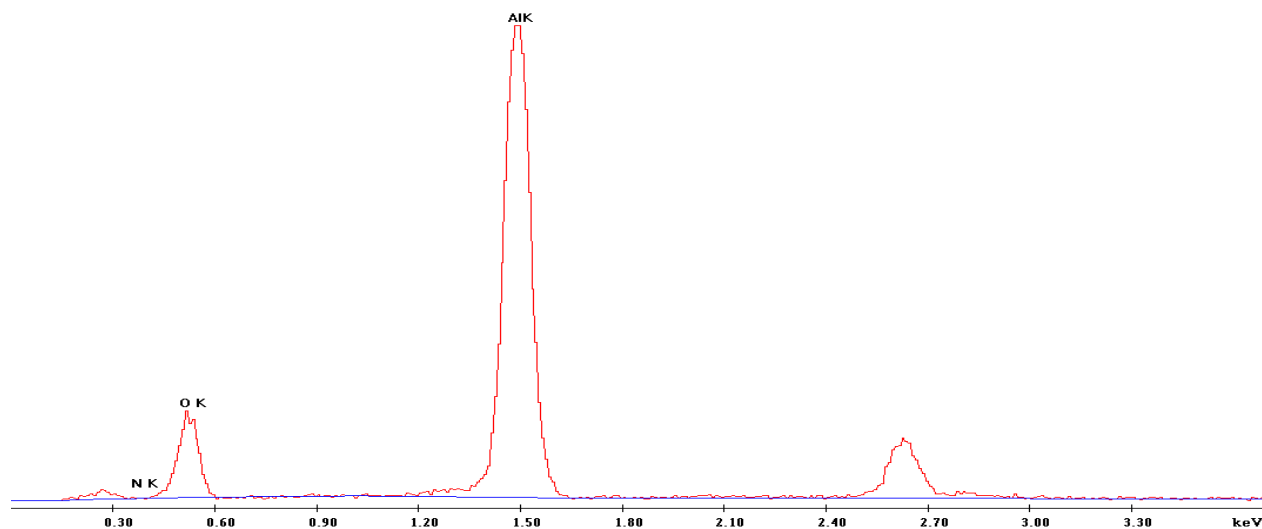
Elem Wt % at % K-Ratio Z A F

```
-----
N K 2.08 3.08 0.0049 1.0480 0.2244 1.0017
O K 41.63 53.80 0.1536 1.0395 0.3546 1.0008
AlK 56.28 43.13 0.4211 0.9681 0.7729 1.0000
Total 100.00 100.00
```

Fig 4.18 Percentage of O₂ Conversion for AlH₃ with 30% of CO₂ in Ar

Figure 4.18 shows that when AlH₃ is burned with 30% of CO₂ in Ar, O₂ conversion is 41.63%.

Label A: Chlorite [Nrm.%= 38.86, 20.96, 34.83, 1.14, 3.84, 0.28]



Elem Wt % at % K-Ratio Z A F

N K 0.49 0.77 0.0010 1.0559 0.1972 1.0014

O K 33.00 45.21 0.1143 1.0474 0.3303 1.0010

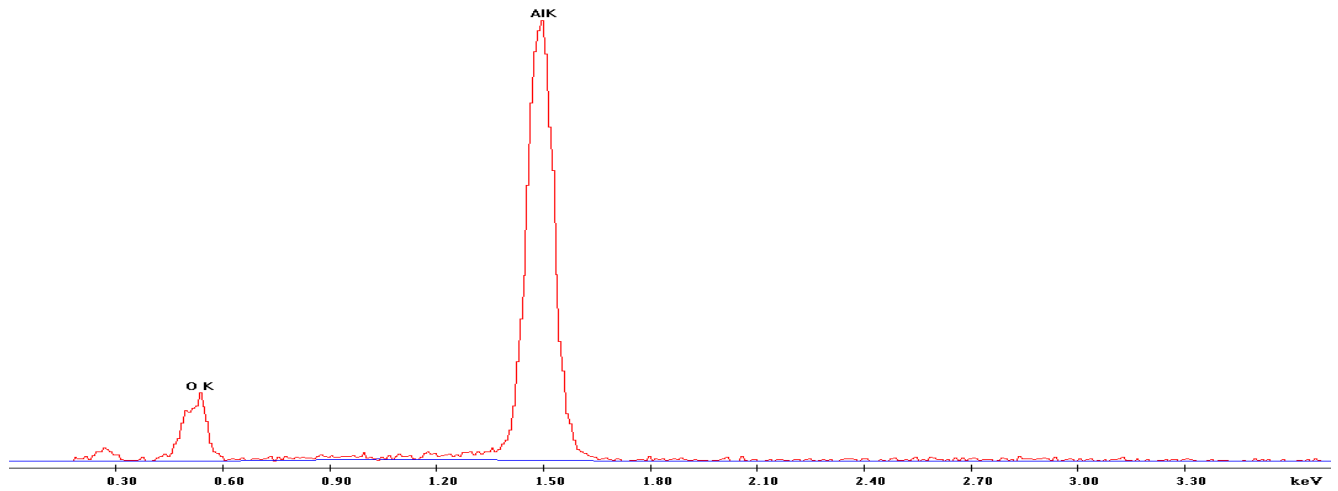
AlK 66.51 54.02 0.5273 0.9754 0.8128 1.0000

Total 100.00 100.00

Fig 4.19 Percentage of O₂ Conversion for Al with 30% of CO₂ in Ar

Figure 4.19 shows that when AlH₃ is burned with 10% of CO₂ in Ar, O₂ conversion is 33%. So the O₂ conversion is higher for AlH₃ than Al with the same volumetric flow rate of oxidizer.

Label A: Chlorite (Nrm.%= 38.86, 20.96, 34.83, 1.14, 3.84, 0.28)



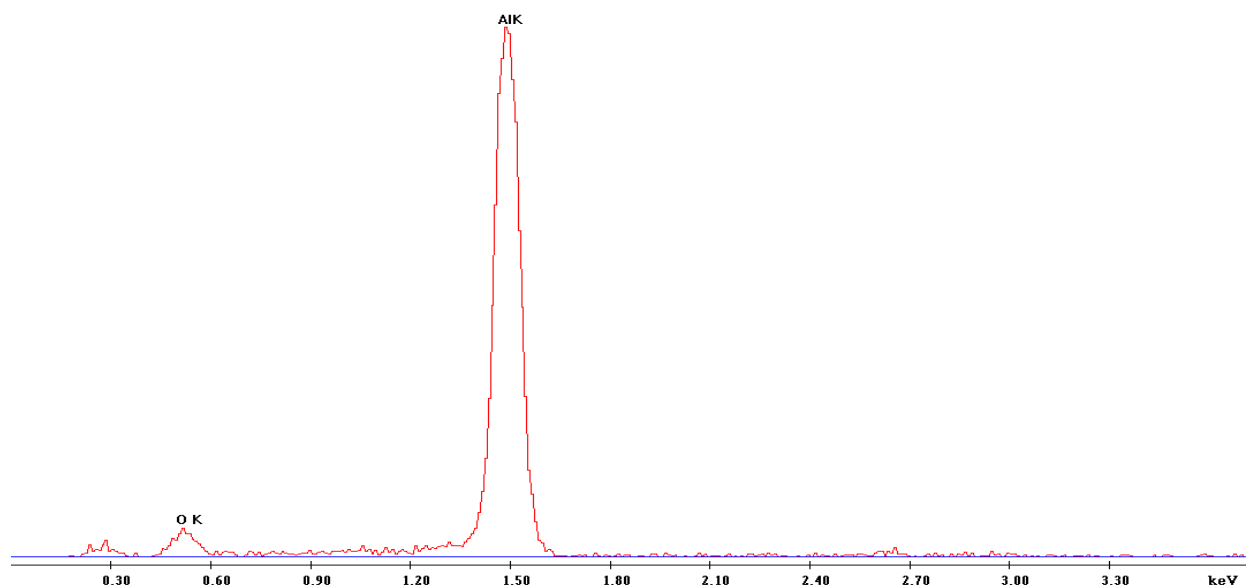
Elem Wt % at % K-Ratio Z A F

O K	24.49	35.36	0.1025	1.0582	0.3949	1.0010
AlK	75.51	64.64	0.6732	0.9798	0.9100	1.0000
Total	100.00	100.00				

Fig 4.20 Percentage of O₂ Conversion for Al H₃ with 40% of CO₂ in Ar

Figure 4.20 shows that when AlH₃ is burned with 30% of CO₂ in Ar, O₂ conversion is 24.49%.

Label A: Chlorite [Nrm.%= 38.86, 20.96, 34.83, 1.14, 3.84, 0.28]



Elem Wt % at % K-Ratio Z A F

O K 11.25 17.61 0.0424 1.0696 0.3520 1.0013

AlK 88.75 82.39 0.8417 0.9906 0.9573 1.0000

Total 100.00 100.00

Fig 4.21 Percentage of O2 Conversion for Al with 40% of CO2 in Ar

Figure 4.21 shows that when Al is burned with 10% of CO₂ in Ar, O₂ conversion is 11.25%. So the O₂ conversion is higher for AlH₃ than Al with the same volumetric flow rate of oxidizer.

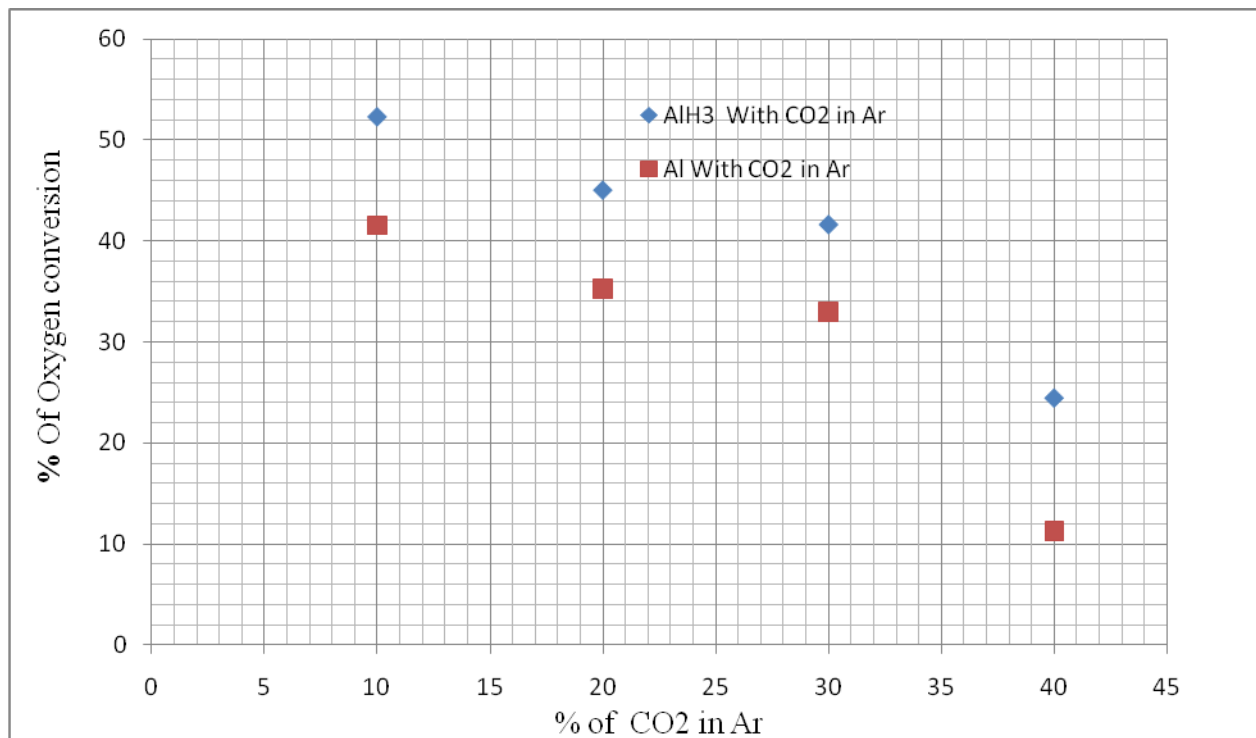


Fig4.22 Percentage of O₂ Conversion for AlH₃ and Al with volumetric flow rate of CO₂ in Ar

Figure 4.22 shows that percentage of O₂ conversion decreases with increasing volumetric flow rate of CO₂ in Ar. And the degree of O₂ conversion is higher for AlH₃ rather than Al. The reason could be the higher proportion of oxidizer relative to fuel.

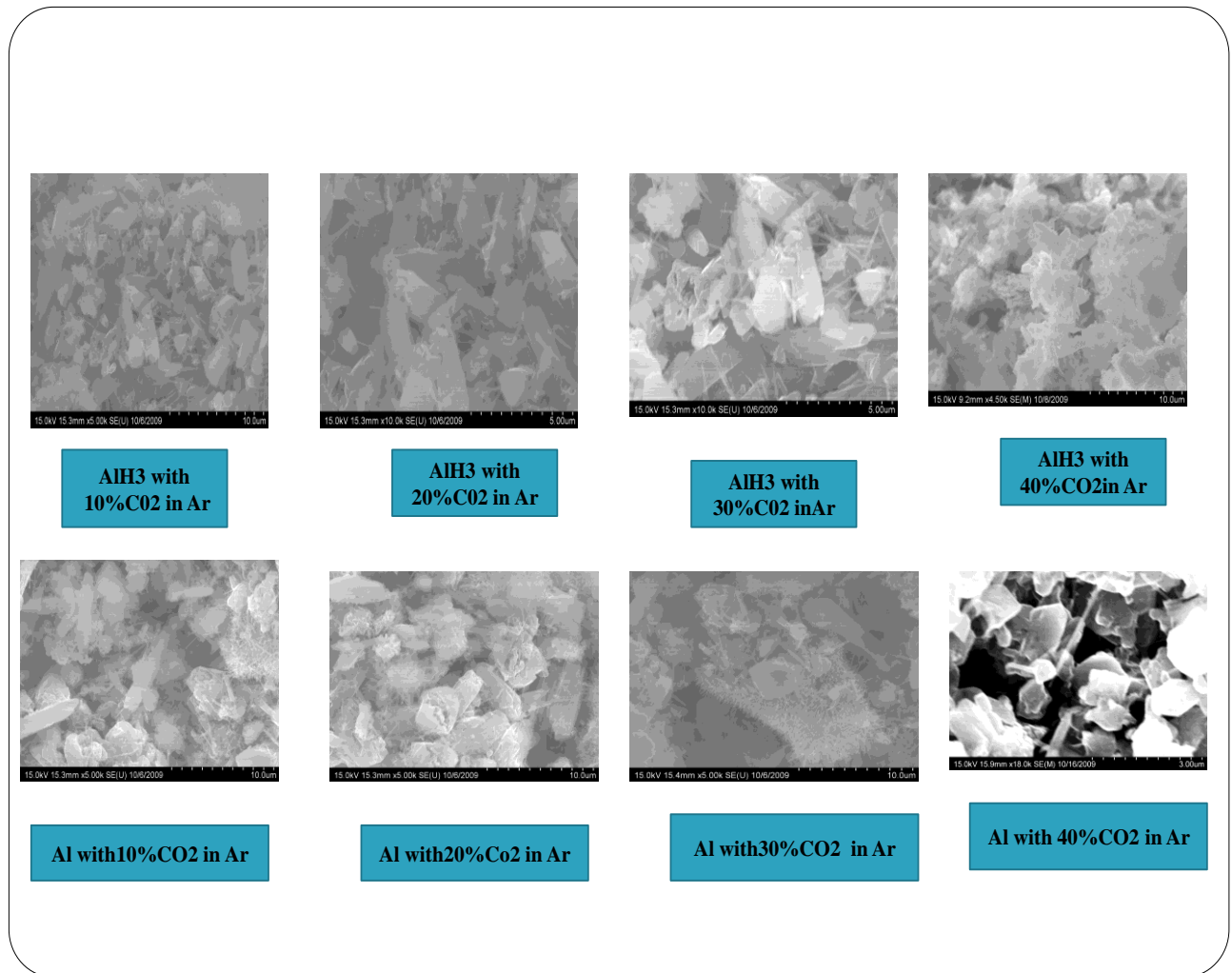


Fig 4.23 SEM images of burned AlH₃ and Al

Figure 4.23 shows that the degree of breaking of pure structure into aggregated and hollow cut structure decreases with increasing the volumetric flow rate of oxidizer. The reason could be the percentage of O₂ conversion decreases with increasing the volumetric flow rate of oxidizer.

4.4 Determination of Minimum Ignition Energy

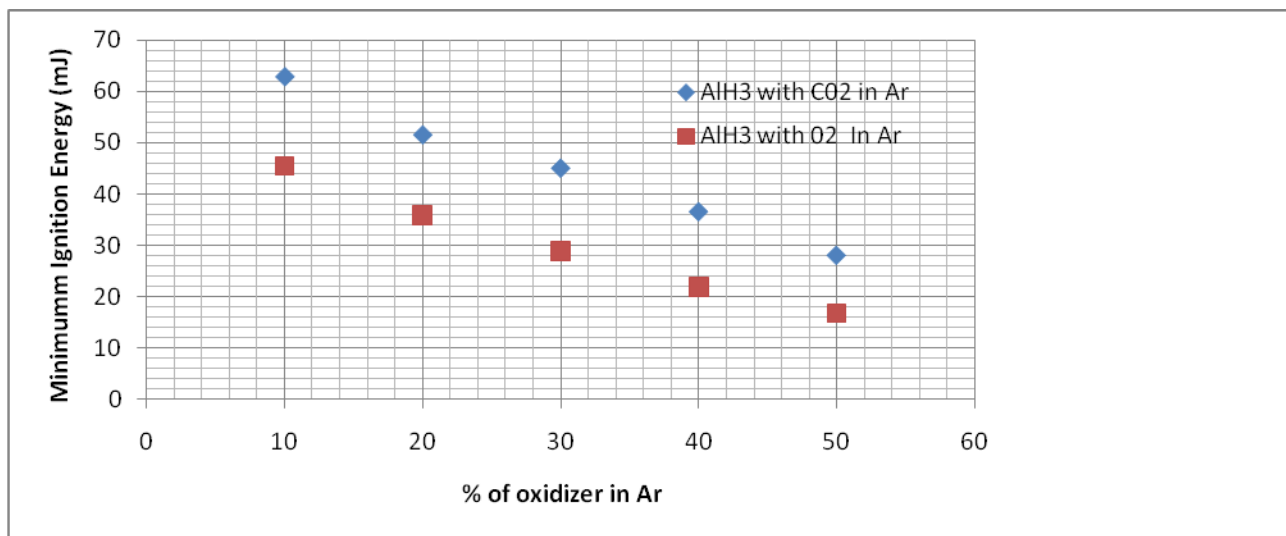


Fig 4.24 Comparison of Minimum Ignition Energy to Burn AlH₃ Using Different Oxidizers (O₂ and CO₂)

Figure 4.24 shows that minimum ignition energy decreases linearly with increasing the volumetric flow rate of oxidizers in Ar for AlH₃. Ignition energy of AlH₃ is higher in CO₂ rather than Al.

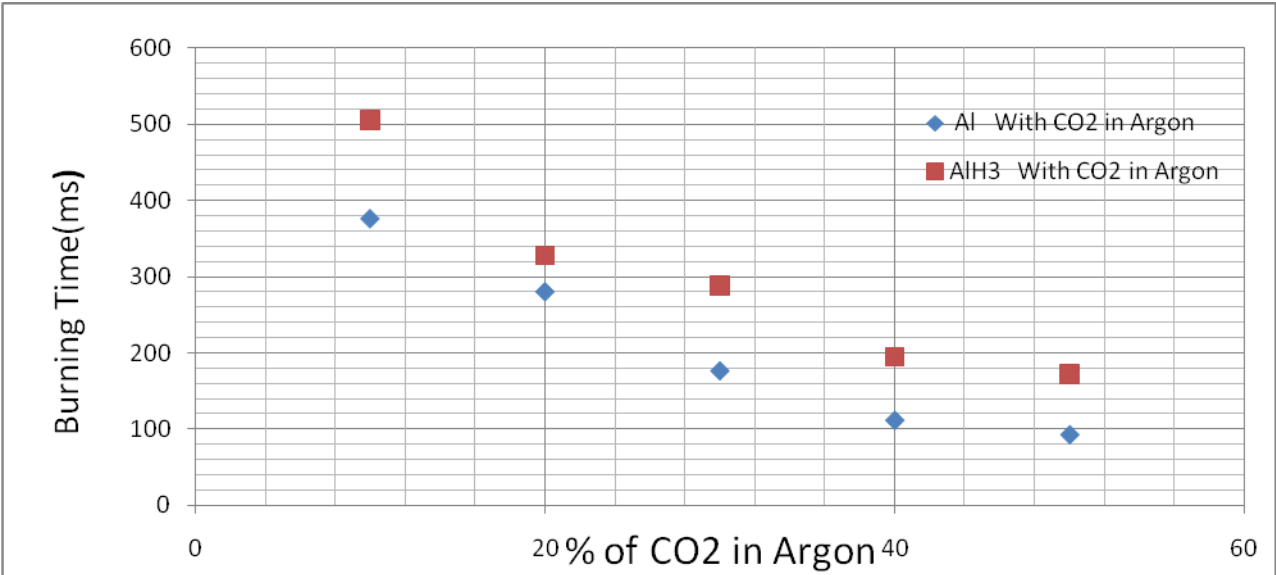


Fig 4.25 Comparison of Minimum Ignition Energy of Al H₃ and Al Using CO₂

Figure 4.25 shows that minimum ignition energy decreases linearly with increasing the volumetric flow rate of oxidizers in Ar for AlH₃ and Al. Ignition energy of AlH₃ is higher than Al.

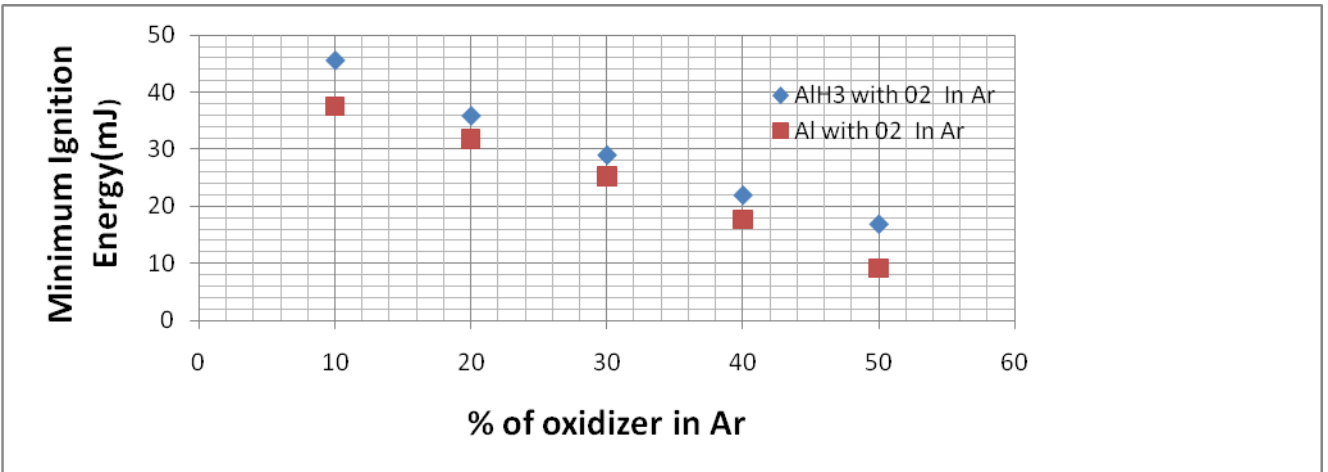


Fig 4.26 Comparison of Minimum Ignition Energy to Burn AlH₃ and Al Using O₂

Figure 4.26 shows that Minimum ignition energy decreases linearly with increasing the volumetric flow rate of oxidizers in Ar for AlH₃ and Al. Ignition energy of AlH₃ is higher than Al

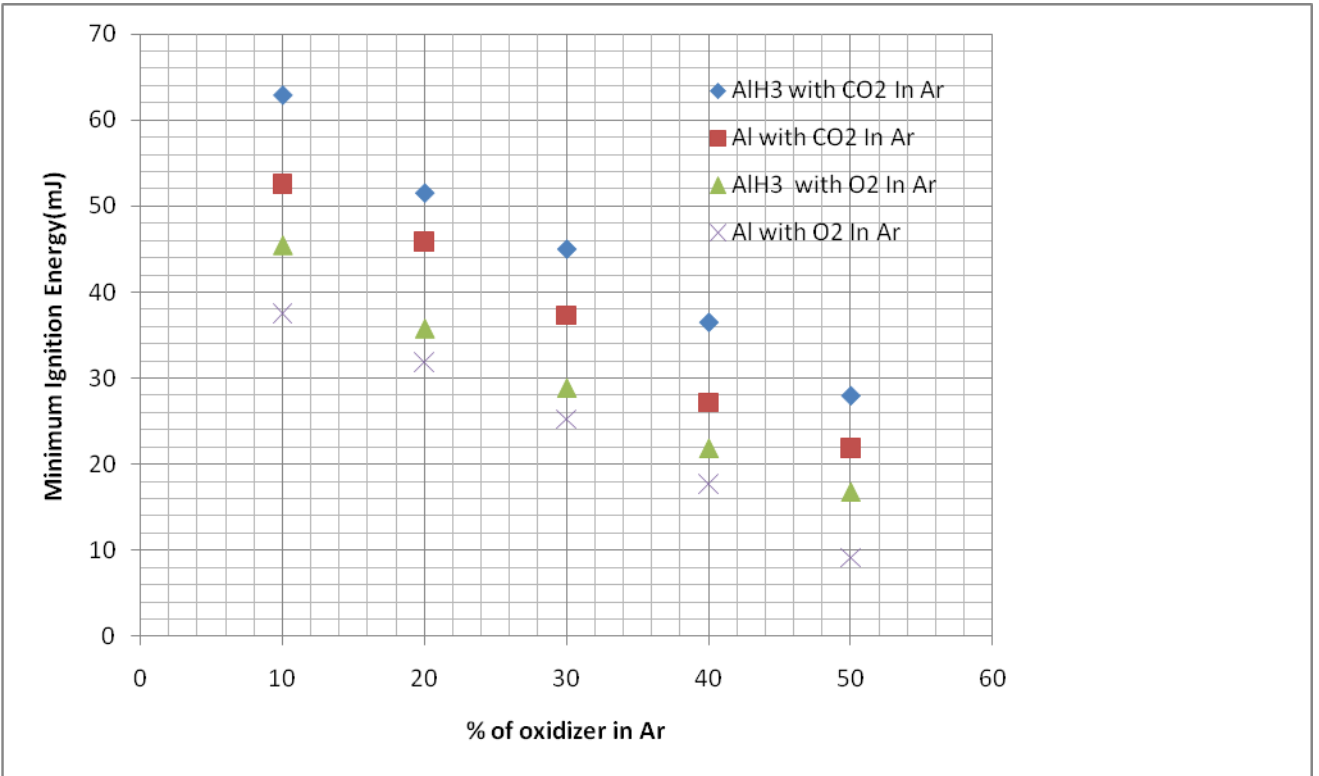


Fig 4.27 Comparison of Minimum Ignition Energy of AlH₃ and Al using Different Oxidizers (O₂ and CO₂)

Figure 4.27 shows that minimum ignition energy decreases linearly with increasing the volumetric flow rate of oxidizers in Ar for AlH₃ and Al. Ignition energy of AlH₃ is higher than Al for all conditions.

4.5 Flame Evolution

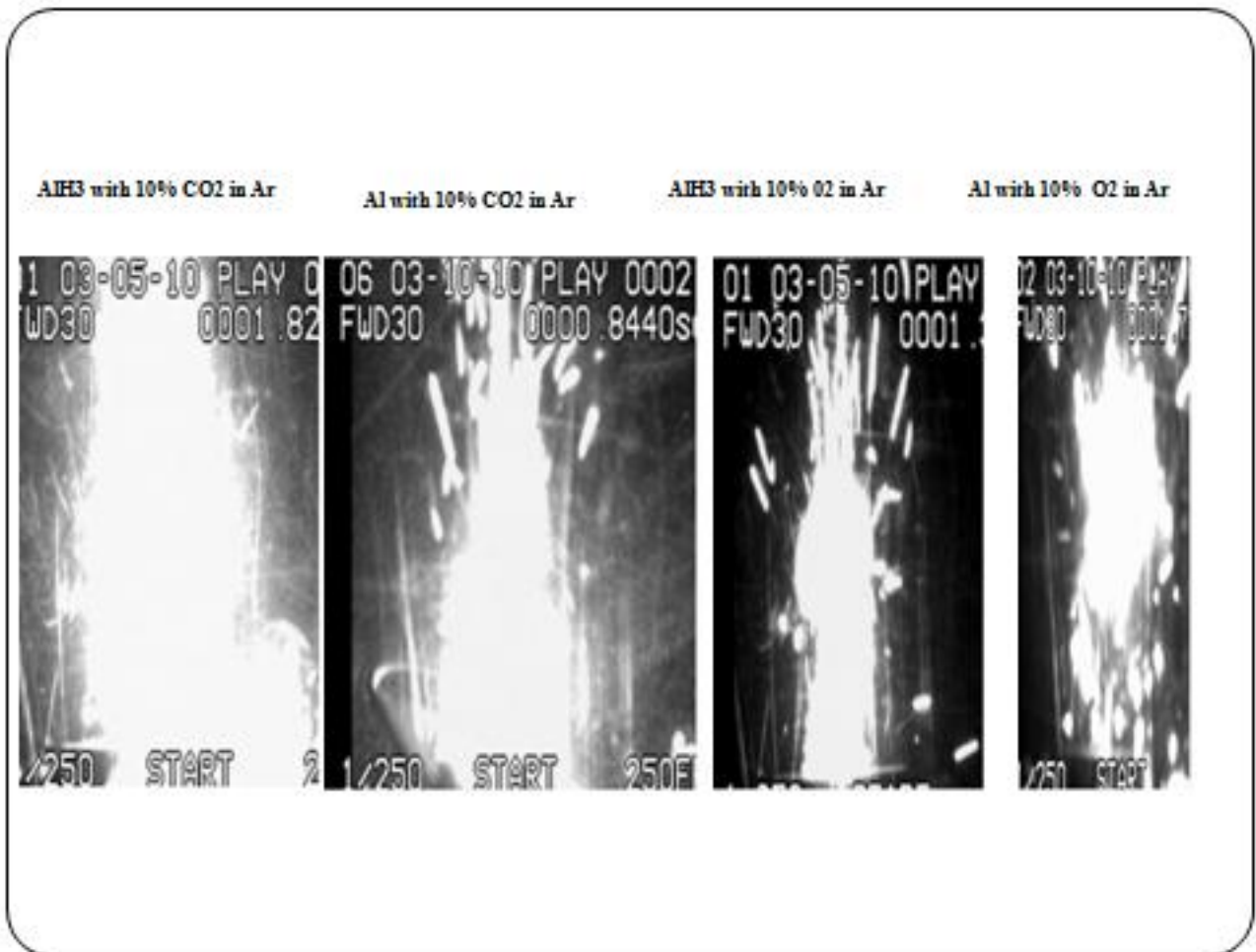


Fig 4.28 Flame Evolution using High Speed Camera

Figure 4.28 shows when AlH₃ burned with 10% of CO₂ in Ar. The quality of the flame structure looks excellent and superior to that of the other images (see Fig. 4.19). The high burning rate favors little agglomeration.

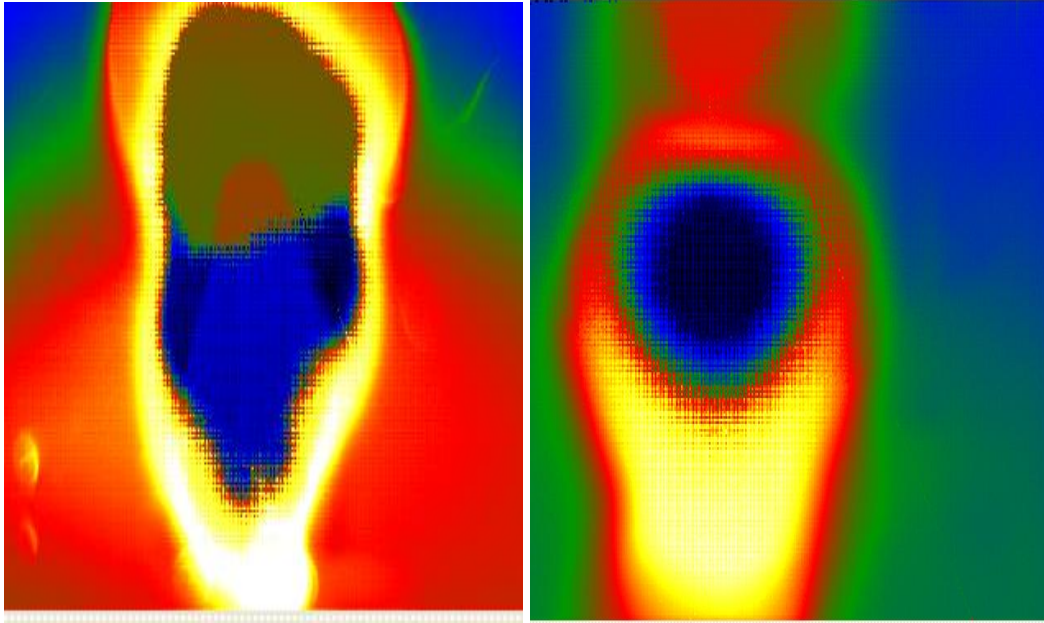


Fig 4.29 (a) AlH₃ Flame with 10% CO₂ in Ar Fig 4.29 (b) Al Flame with 10% CO₂ in Ar

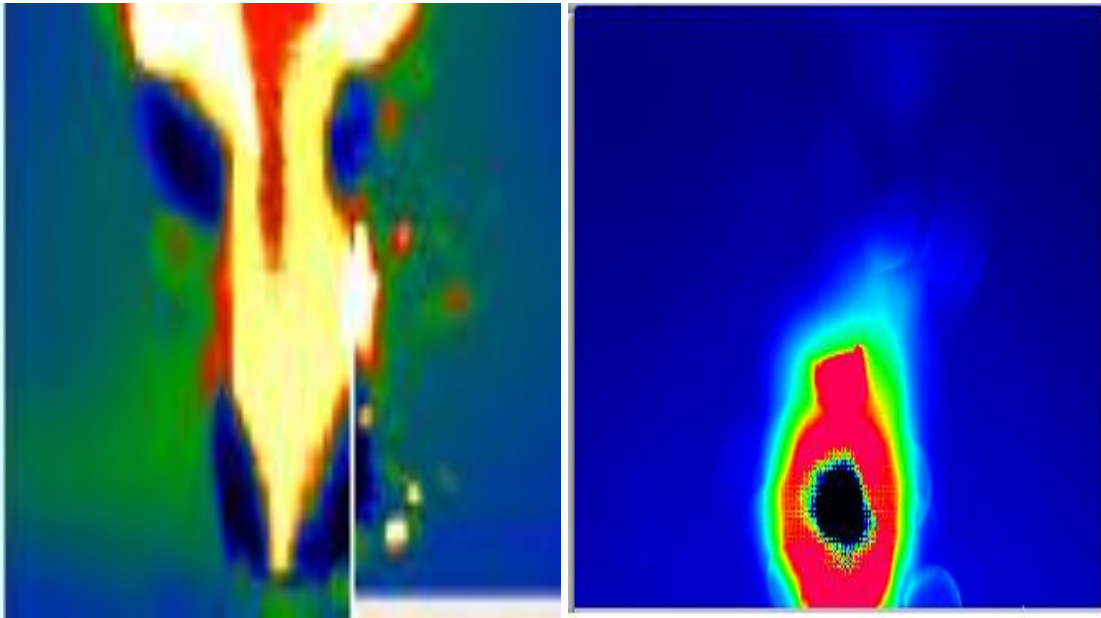


Fig 4.29 (c) AlH₃ Flame with 10% O₂ in Ar Fig 4.29 (d) Al Flame with 10% O₂ in Ar

Flame evaluation using thermal camera suggests that according to spectrum the AlH₃ flame has the warmer zone rather than the Al flame

4.6 Determination of Burning Time Using Emission Spectra of AlO

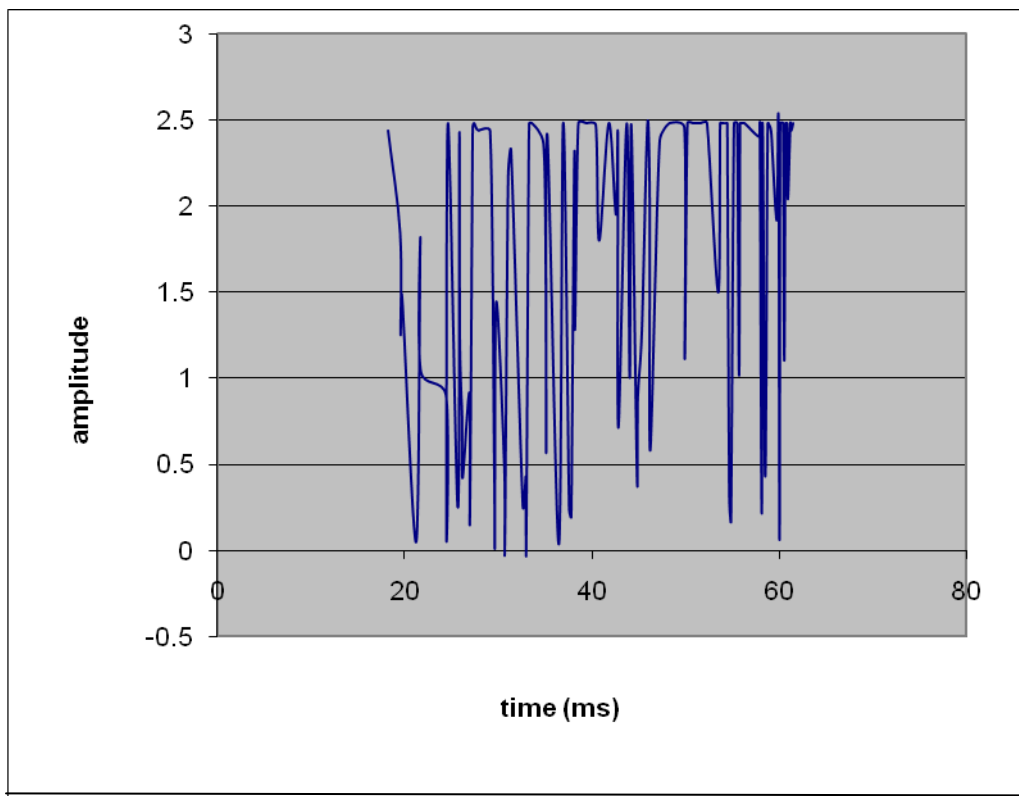


Fig 4.30 Emission Spectra of AlH₃ Flame using 10% CO₂ in Ar

The emission spectra were measured at 486 nm wavelength. Emission spectra shows that when AlH₃ is burned with 10% of CO₂ in Ar, the duration of flame stabilization is from 21.5-60 ms, which does not match with the value taken from high speed camera. The probable reason is discussed in the conclusions section.

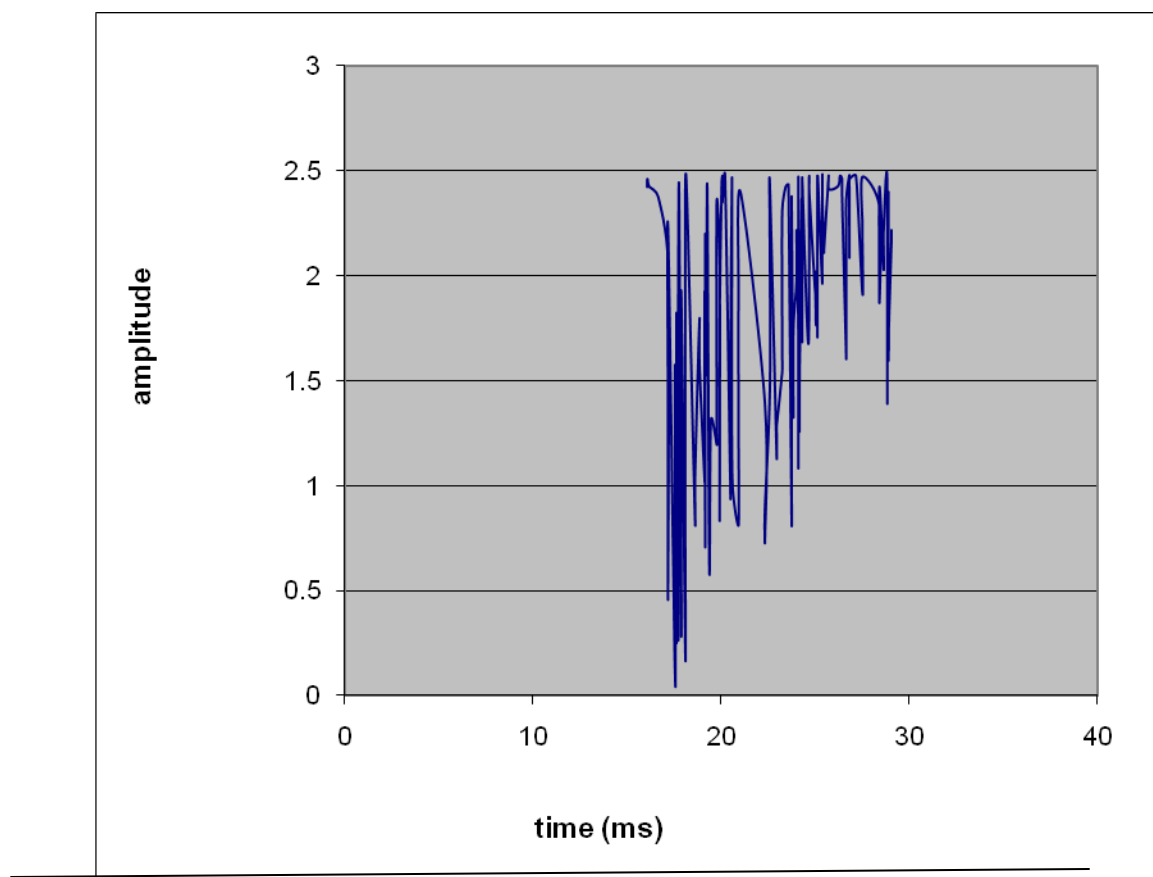


Fig 4.31 Emission spectra of Al flame using 10% CO₂ in Ar

The emission spectra were measured at 486 nm wavelength. Emission spectra shows that when Al is burned with 10% of CO₂ in Ar, the duration of flame stabilization is from 18-29 ms, which does not match with the value taken from high speed camera. The probable reason is discussed in the conclusions section.

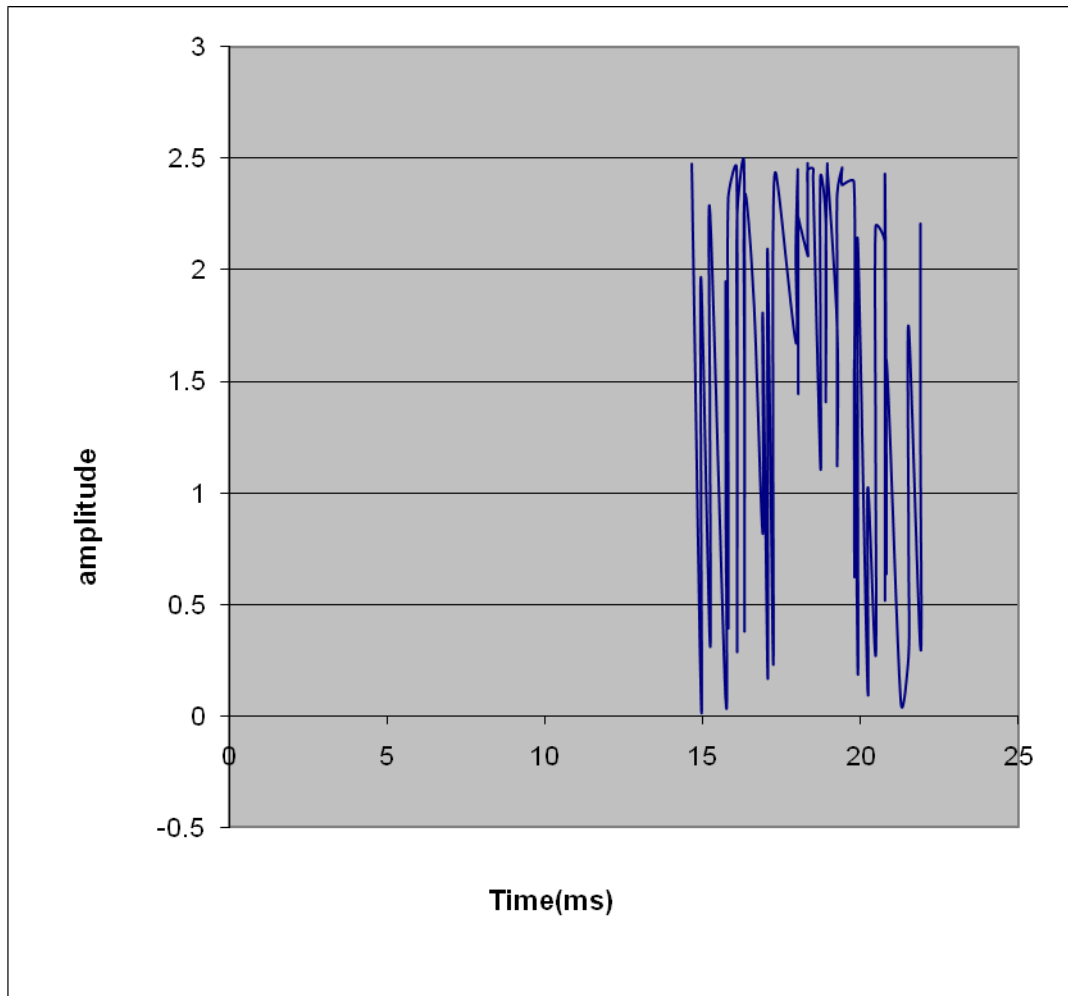


Fig 4.32 Emission spectra of AlH₃ and Al flame using 20% CO₂ in Ar

The emission spectra were measured at 486 nm wavelength. Emission spectra shows that when AlH₃ and Al burned with 10% of CO₂ in Ar, the duration of flame stabilization is from 15-21.5 ms, which does not match with the value taken from high speed camera. The probable reason is discussed in the conclusions section.

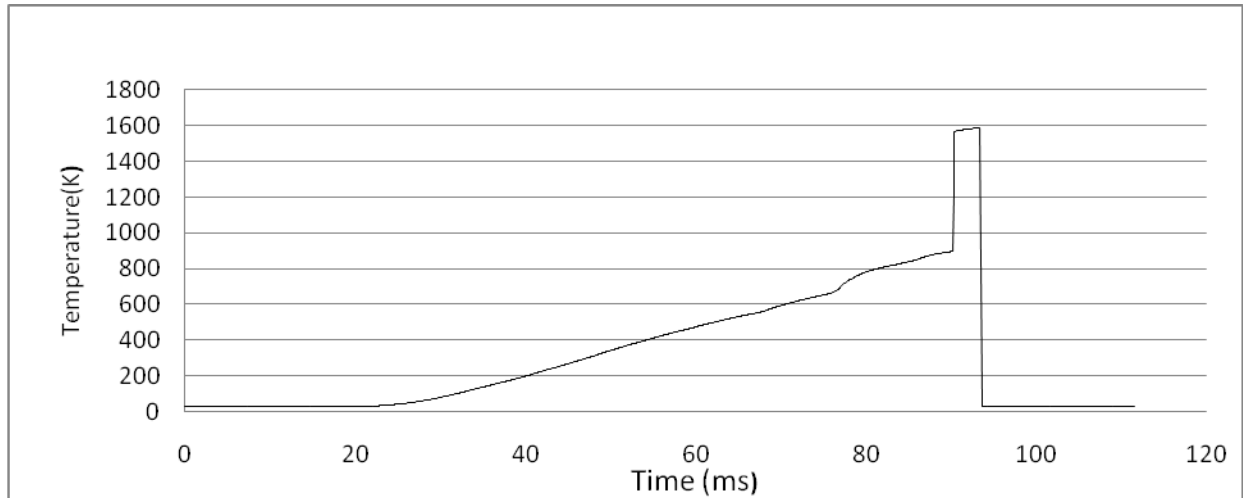


Fig 4.33 (a) Temperature of AlH₃ flame using 50% CO₂ in Ar

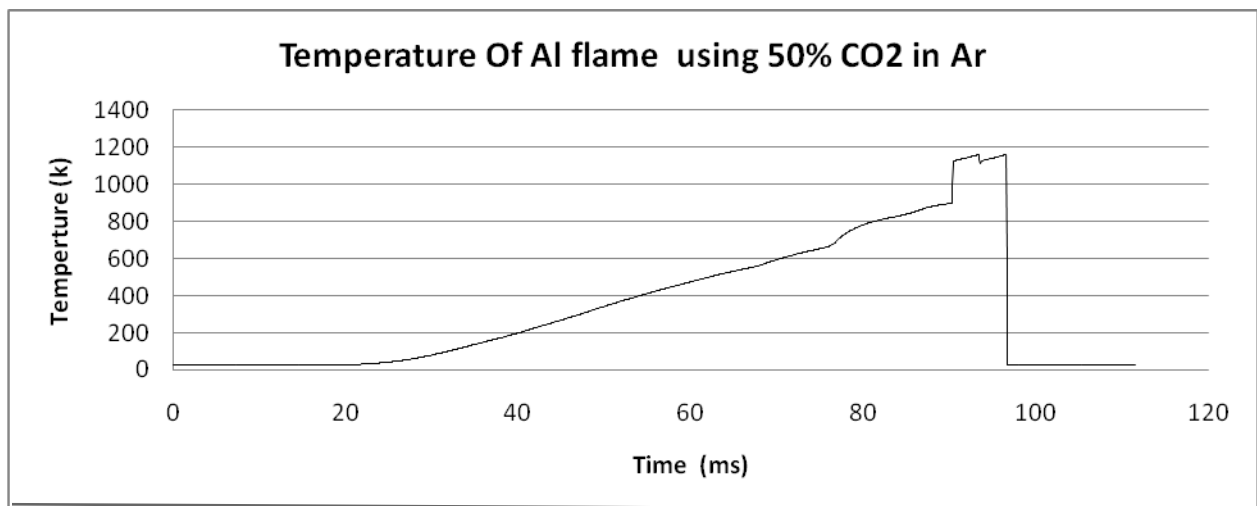


Fig 4.33 (b) Temperature of Al Flame using 50% CO₂ in Ar

Figures 4.33(a) and 4.33(b) show that flame temperature of AlH₃ is higher than Al for the same volumetric flow rate of oxidizer.

5.0Conclusions

1. Scanning Electronic microscopic images of sample (AlH₃ and Al) reveals the morphology of the pure sample.

2. EDAX analysis of the sample indicates that the sample, AlH₃, contains only 5 percent of O₂ and Al contains no O₂ content, which is the best indication of pure sample.

3. Burning time (using high speed camera) decreases almost linearly with increasing the volumetric flow rate of oxidizers in Ar for AlH₃ and Al. Burning time of AlH₃ is higher than Al for all conditions. A brief table is given below

Al with CO ₂ in Ar	
% of CO ₂ in Ar	Burning Time(mS)
10	376
20	280
30	176
40	111
50	92

Al H ₃ with O ₂ in Ar	
% of CO ₂ in Ar	Burning Time(mS)
10	228
20	168
30	124
40	80
50	64

Al with CO ₂ in Ar	
% of CO ₂ in Ar	Burning Time(ms)
10	376
20	280
30	176
40	111
50	92

Al with O ₂ in Ar	
% of CO ₂ in Ar	Burning Time(ms)
10	168
20	128
30	100
40	36
50	20

4. Minimum ignition energy decreases linearly with decreasing burning rate for AlH₃ and Al. Ignition energy of AlH₃ is higher than Al for all conditions. A brief table is given below.

Al with CO₂ in Ar

% of CO ₂ in Ar	Minimum Ignition Energy (mJ)
10	62.9
20	51.54
30	45.03
40	36.52
50	28

AlH₃ with O₂ in Ar

% of CO ₂ in Ar	Minimum Ignition Energy (mJ)
10	45.51
20	35.8
30	28.9
40	21.86
50	16.78

Al with CO ₂ in Ar	
% of CO ₂ in Ar	Minimum Ignition Energy (mJ)
10	52.54
20	45.88
30	37.33
40	27.2
50	21.86

Al with O ₂ in Ar	
% of CO ₂ in Ar	Minimum Ignition Energy (mJ)
10	37.52
20	31.84
30	25.25
40	17.73
50	9.15

5. Percentage of conversion of O₂ during combustion of AlH₃ and Al decreases non linearly with decreasing the burning time. A brief table is given below.

AlH₃ With CO₂ in Ar

% of O ₂ in Ar	% of O ₂ conversion
10	52.27
20	45.03
30	41.63
40	24.49

Al With CO₂ in Ar

% of O ₂ in Ar	% of O ₂ conversion
10	41.55
20	35.26
30	33.00
40	11.25

6. Since the combustion properties of AlH₃ are better than Al, so the replacement of Al with AlH₃ in energetic materials applications would be significantly facilitated

References

- [1] Graetz Jason, J Reilly James, Johnson, G. Sandrock, John, Zhou, Wei Min Zhou and Wegrzyn James," Aluminum Hydride, AlH_3 , As a Hydrogen Storage Compound", Brookhaven National Laboratory, BNL-77336-2006
- [2] Bazyn, T., Eyer, R., Krier,H., andGluma, N., "Combustion Characteristics of Aluminum Hydride at Elevated Pressure and Temperature",Mechanical and Industrial Engineering Department University of Illinois at Urbana-Champaign,Urbana, IL 61801
- [3] Sinke, G. C.; Walker, L. C.; Oetting, F. L.; Stull, D. R. J. Chem. Phys. 1967, 47, 2759
- [4] Baranowski, B.; Tkacz, M. Z. Phys. Chem. 1983, 135, 27.
- [5] Lund, Gary K., Hanks, Jami M., Johnston, Harold E., US Patent and Trade Office, **2007**, Pat. Application # 20070066839
- [6] Turley J W,. Rinn H W (1969). "The crystal structure of Al hydride". *Inorganic Chemistry* **8** (1)18–22doi:[10.1021/ic50071a005](https://doi.org/10.1021/ic50071a005)
- [7] Sarner SF. Propellant Chemistry, Reinhold Publishing Corporation, 1966.
- [8] Thome V, Kempa PB, and Herrmann M. Structure, chemical and physical behavior of Al hydride, Proceedings ICT 2003, Paper P-104, 2003..
- [9] Chan ML and Johnson CL. Evaluation of AlH_3 for propellant application, Proceedings 8-IWCP, edited by L.T. DeLuca, Grafiche GSS, Bergamo, Italy, Paper 33, 2003.
- [10] Thome V, Kempa PB, and Herrmann M. Structure, chemical and physical behavior of Al hydride, Proceedings ICT 2003, Paper P-104, 2003.
- [11] Selezenev, A. A., Kreknnin, D. A., Lashkov, V. N., Lobanov, V. N., and Fedorov, A. V., “Comparative Analysis of the Effects of Aluminum and Aluminum

Hydride on the Detonation Parameters and Performance of Mixed Explosives,”
Proceedings of the 11th International Detonation Symposium, Snowmass, CO, 1998, pp.
231-236.

[12] Il'in, A.P., Bychin, N.V., and Gromov, A.A., “Products of Combustion of
Aluminum Hydride in Air,” Combustion, Explosion, and Shock Waves, Vol. 37, No. 4,
2001, pp. 490-491.

[13] F.M. Brower, N.E. Matzek, P.F. Reigler, H.W. Rinn, C.B. Roberts, D.L. Schmidt, J.A.
Snovar, K. Terada, J. Am. Chem. Soc. 98 (9) (1976) 2450–2453

[14] Ngo, My, "Determination of the minimum ignition energy (mie) of premixed propane/air",
Department of Physics and Technology, University of Bergen, Norway, June 2009

Curriculum Vita

Sudipa Sarker was born February 18, 1981 to Rakesh Chandra Sarker and Kanan Sarker. She graduated with a Mathematics and Science Degree at the Govt Women's College (Sylhet Bangladesh) in 1999. In 2006, she received her Bachelor's of Science Degree in Chemical Engineering and Polymer Science from Shahjalal University of Science and Technology, Bangladesh. Ultimately, she completed her Master's of Science Degree in Mechanical Engineering in 2010, focusing her research in the Center for Space Exploration Technology Research (formerly Combustion and Propulsion Research Lab) under the guidance of Dr. Ahsan Choudhuri, Ph.D.

Permanent address: 1118 Los Angeles Dr. Apt#5

El Paso, TX-79902, USA

This thesis was typed by Sudipa Sarker